ARGONNE NATIONAL LABORATORY
9700 South Cass Avenue
Lemont, IL 60439

Optimal Design and Dispatch of a System of Diesel Generators, Photovoltaics and Batteries for Remote Locations

Michael S. Scioletti, Alexandra M. Newman, Johanna K. Goodman, Alexander J. Zolan, and Sven Leyffer

Mathematics and Computer Science Division

Preprint ANL/MCS-P7037-0417

April 10, 2017

This work was supported by the U.S. Department of Energy, Office of Science, Office of Advanced Scientific Computing Research, under Contract DE-AC02-06CH11357.

Contents

Optimization and Engineering manuscript No.
(will be inserted by the editor)

Optimal Design and Dispatch of a System of Diesel Generators, Photovoltaics and Batteries for Remote Locations

Michael S. Scioletti · Alexandra M. Newman · Johanna K. Goodman · Alexander J. Zolan · Sven Leyffer

DRAFT as of April 10, 2017

Abstract Renewable energy technologies, specifically, solar photovoltaic cells, combined with battery storage and diesel generators, form a hybrid system capable of independently powering remote locations, i.e., those isolated from larger grids. If sized correctly, hybrid systems reduce fuel consumption compared to diesel generator-only alternatives. We present an optimization model for establishing a hybrid power design and dispatch strategy for remote locations, such as a military forward operating base, that models the acquisition of different power technologies as integer variables and their operation using nonlinear expressions. Our cost-minimizing, nonconvex, mixed-integer, nonlinear program contains a detailed battery model. Due to its complexities, we present linearizations, which include exact and convex under-estimation techniques, and a heuristic, which determines an initial feasible solution to serve as a "warm start" for the solver. We determine, in a few hours at most, solutions within 5% of optimality for a candidate set of technologies; these solutions closely resemble those from the nonlinear model. Our instances contain real data spanning a yearly horizon at hour fidelity and demonstrate that a hybrid system could reduce fuel consumption by as much as 50% compared to a generator-only solution.

M. Scioletti · A. Newman
Department of Mechanical Engineering, Colorado School of Mines, Golden, CO 80401
E-mail: msciolet@mines.edu, E-mail: anewman@mines.edu
J. Goodman
School of Chemical and Biomolecular Engineering, Georgia Institute of Technology, Atlanta, GA 30332
E-mail: gtpaddle@gmail.com
A. Zolan
Department of Mechanical Engineering, University of Texas at Austin, Austin, TX 78712
E-mail: alex.zolan@utexas.edu
S. Leyffer
Mathematics and Computer Science Division, Argonne National Laboratory, Lemont, IL 60439 E-mail: leyffer@mcs.anl.gov

1 Introduction and Literature Review

Hybrid power systems integrate renewable energy technologies, such as solar photovoltaic devices (PV), with energy storage systems (batteries) and diesel generators to provide grid-quality electrical power to remote locations. If sized and operated efficiently, hybrid systems are a cost-beneficial alternative to grid extension and spot generation. To this end, we construct a mixed-integer, nonlinear optimization model that determines the number and type of PV, battery, and generator technologies to procure, and how to operate them on an hourly basis so as to minimize costs, while adhering to constraints that govern the operation of the system. Because nonlinearities lead to tractability issues, we present linearizations that yield good approximations to the nonlinear model. We also assume that our inputs are deterministic. While even higher fidelity models may be formulated, our goal is to make design decisions, and to use the dispatch as a guide for these decisions [29]. Real-time dispatch would require a more detailed model, taking the design as fixed. Our load profiles demonstrate significant variability over the course of one year, and this serves as a proxy for making our design decisions robust to stochastic loads. Furthermore, as we discuss throughout the paper, even our one-stage deterministic model is associated with instances that are difficult to solve; our proposed techniques enhance that solvability, and, to our knowledge, demonstrate current state of the art. Accounting for stochasticity with a two- or multi-stage approach would result in an intractable model.

Optimally determining design and dispatch is an NP-hard problem that involves modeling nonlinearities and integer restrictions. It is common to separate the problem into one of (i) design or (ii) dispatch and then solve; however, this does not guarantee global optimality of the solution, because it is a restriction of the problem. Our computational tests show that, for our instances, basing an entire design and dispatch solution simply on a design that examines maximum load can result in solutions that use 50% more fuel. More tailored heuristics show promise in providing good, but not optimal, results to the design problem [37, 15, 14, 38, 25], but often rely on dispatch strategies set a priori ([13] and [17]) to satisfy demand constraints. Some authors use multiple objectives such as cost, reliability, and emissions reduction or Pareto optimality assessment techniques as part of a heuristic strategy [19], but have difficulty establishing solution quality. Shortening the time horizon [43] and/or reducing the variability in daily demand [19] increases tractability of the problem; however, seasonal changes in demand could significantly impact design decisions.

HOMER (Hybrid Optimization Model for Electric Renewables), at the time of this writing, is the most widely used design and dispatch program [36, 48, 53, 31, 41] and represents a simulation model that, for a year-long demand profile, uses fixed dispatch strategies and ranks resulting solutions based on life-cycle cost [8]. Few modeling efforts include deterministic methods such as linear programming (LP) and/or mixed integer programming (MIP) to solve the design and dispatch problem, especially as a monolith for a year-long hori-

zon with hourly time fidelity. A MIP with wind power, batteries, and generators [16] produces results comparable to HOMER's; however, it fails to address the complexities associated with battery modeling and solves the problem in two steps: (i) design solutions result from running the MIP for a curtailed time horizon and then (ii) dispatch solutions follow for the entire year given design from (i). A linear program solves a year-long problem at hourly time fidelity to understand the operating relationships between the technologies within a hybrid system over a 20-year ownership timeline [33]; but, the model considers identical 24-hour demand periods for the entire year and lacks battery modeling detail. Given the unpredictability of renewable energy, [10] presents a stochastic model to account for the variations in windspeed by solving a year-long problem decomposed into day-long, i.e., 24-hour, sub-problems; however, the authors fix technologies in their hybrid system with the goal of optimizing the sizing of an energy storage system, which could consist of batteries, flywheels, and supercapacitators [9]. Alternately, [46] develops a nonconvex mixed-integer, nonlinear program (MINLP) to describe the design and dispatch of a distributed combined heat and power generation system using Solid Oxide Fuel Cells (SOFC), PV, and batteries for commercial buildings for a time horizon of one year (8,760 hours). Due to the complexities of modeling SOFCs, the authors do not attempt to model batteries or PV in detail. By developing a convex under-estimation of the MINLP through a linearization technique for bi- and tri-linear terms, the authors present a MIP that, with the help of a bounding algorithm which takes days to run, solves year-long instances to a gap less than 8%.

Through the use of a heuristic, which serves to provide the solver with an initial feasible solution and linearizations, which include exact and convex under-estimation techniques, our research contributes to the literature by solving the design and dispatch problem to within 5% of optimality given a candidate set of technologies in a matter of hours for a year-long demand forecast with hourly fidelity. Attributes that differentiate our model from those in the literature include: (i) nonlinearities associated with modeling battery discharge and lifetime; (ii) realistic procurement technology sets with varying sizes and quantities, i.e., a design; and (iii) an unbiased dispatch strategy reflective of demand in each time period. Without loss of generality, we apply our model to forward operating bases (FOBs), though it could also be used in a variety of other microgrid situations.

The remainder of this paper is organized as follows: Section 2 presents the formulation of the MINLP, which includes the linearization techniques and subsequent re-formulation of the problem as a MIP, while Section 3 introduces heuristics to reduce the size of the problem and produce an initial feasible solution. In Section 4, we discuss instances for different demand profiles used to test the MINLP and MIP models; examine the mathematical characteristics and methods to solve both problems; and discuss their results and accuracy. Section 5 concludes.

2 Model

Our model includes two types of variables: design and dispatch, i.e., the levels at which the procured technologies operate to meet a prescribed demand profile for one year at an hourly time fidelity. We minimize procurement, fuel, and lifecycle costs subject to load, capacity and system interoperability constraints.

2.1 Model Overview

A hybrid system incurs capital costs that originate from commercial prices and availability, and operational costs, including those for fuel. We assume that the hybrid system operates independently of a commercial grid (see Figure 1) and can consist of multiple component sizes within each technology and/or of more than one of the same size technology. PV panels form an array, while generators are located adjacent to each other. Batteries of like type comprise a bank that operates as a single unit to preclude modeling individual cells, which would increase the size of the problem. PV technologies first connect to a DC-to-DC converter for the purpose of maximum power point tracking, which links to a bi-directional converter, while battery technologies connect directly to the bi-directional converter. Generator technologies connect directly to the AC bus, which connects to the power demand. We only implicitly model the bus system and the bi-directional converter through their efficiencies.

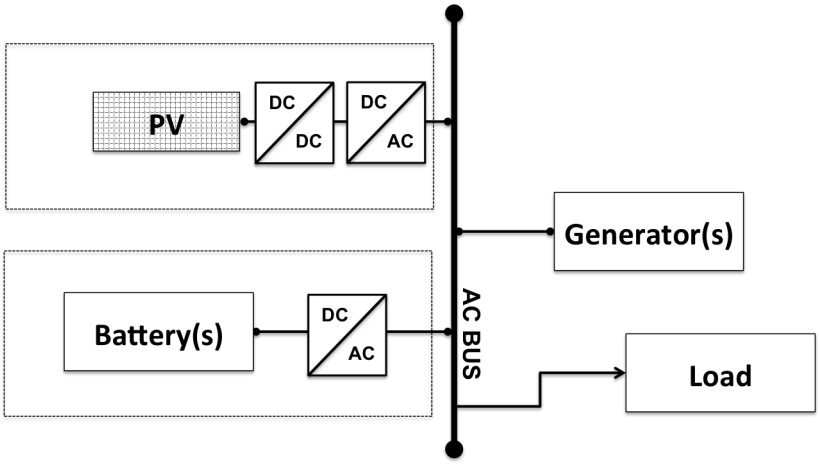

Fig. 1: A topological layout of the proposed hybrid system that includes generator, PV, and battery technologies. All technologies are physically located in close proximity to each other.

The model acquires technologies and then assigns a fraction of the load to each in order to supply enough power to meet the demand in each time period. To allow for the acquisition of a variety of generator types, we do not constrain generators to equally share the load or to operate in droop. Power from the generators both meets demand and charges the battery so long as the generator operates within bounds prescribed by the manufacturer. We model the lifetime of the generator by counting the number of hours it is in operation. A generator's fuel consumption is related quadratically to its power output, but manufacturer data often implies a linear relationship (see Figure 2), in which the intercept is greater than zero.

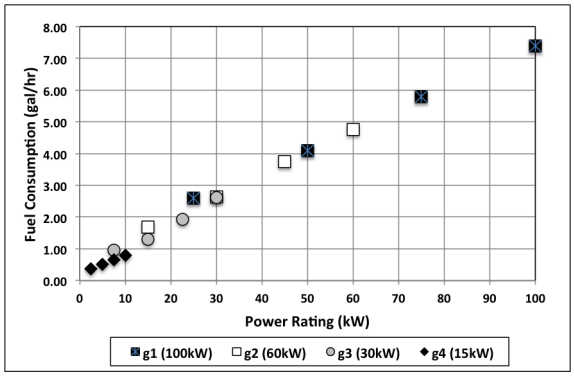

Fig. 2: Manufacturer-provided fuel consumption data points for four differently sized generator technologies [3]. We use a_g^f, b_g^f, and c_g^f to model the quadratic fit.

We model PV power output using NREL's PVWatts panel calculator. A PVWatts simulation model maps solar irradiation based on location, and simulates power output of a PV panel at hourly fidelity for time horizons up to one year [23]. Although PV panel power output is a direct current (DC), PVWatts outputs an alternating current (AC) that accounts for power conversion losses from the hybrid system. If stored, which occurs when PV power is greater than demand, PV power is subject to efficiency losses related to battery charging. A PV array requires space, which we restrict by area, or number of panels. We account for the intermittent nature of PV power by maintaining a spinning reserve capability through a battery's state of charge (SOC), i.e., a measure of its available capacity, and/or by operating generators at less than their rated power. Spinning reserve constraints in design and dispatch problems often consider the economics associated with buying and selling electricity to a grid [45, 32, 44, 47]; however, the remote hybrid system problem is grid-independent, so we model spinning reserve as a fraction of PV power output to account for the variability of the latter within each hour-long time period.

Aside from the load, charging the batteries is the only power draw on the system. Batteries provide power to meet the load, but are also employed as a reserve for the renewable technologies. We do not allow a battery to charge and discharge in the same time period. Power output from a battery is a function of the nonlinear relationship between current and voltage; models that consider this relationship are more accurate than those that do not for many battery chemistries [51]. The current depends on a battery's SOC. Batteries show a rate-capacity effect, in which the available capacity based on the SOC decreases with higher current draw.

Figure 3a displays battery voltage as a function of SOC for a fixed discharge and charge current [1]. By slightly restricting the SOC operating range, we can model the voltage using a linear relationship between SOC and current. Common to most batteries is a rate-capacity effect, which implies that as the magnitude of the discharge current increases, the available capacity decreases. Peukert's equation is often used to describe this behavior [24]. This concept is also employed by [39]'s kinetic energy battery model, which relates the change in capacity to the charge and discharge rates using a two-tank model. While the rate-capacity effect is nonlinear over a large current range, especially at high currents, our hourly time step allows us to use a linear approximation over the relevant current range (see Figure 3b).

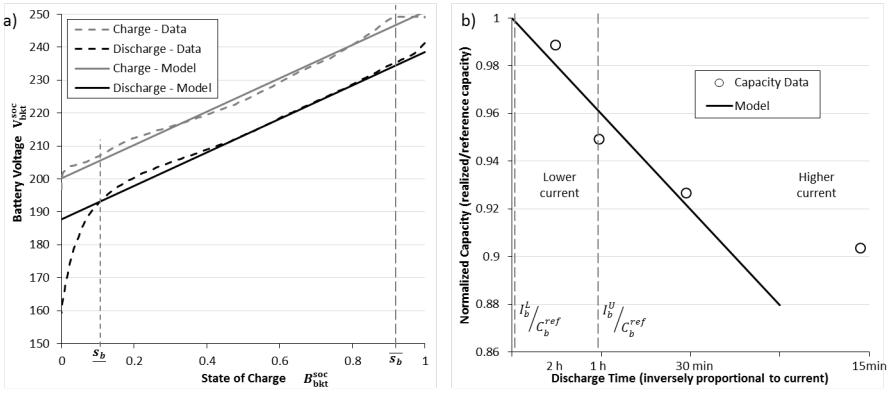

Fig. 3: A graphical comparison of a) battery voltage for a battery b, "twin" k, and time period t, V_{bkt}^{soc} as a function of state of charge B_{bkt}^{soc}, for which we use a_b^v and b_b^v to represent the slope and intercept, respectively, where the intercept is augmented by constants representing Ohm's law (see constraint (5g)); and b) the normalized capacity, which we model as the quotient of the maximum realized current I_b^U and capacity c_b^{ref} of a battery given discharge time.

We account for battery chemistry characteristics such as the voltage and rate-capacity behavior, but exclude chemistry-specific aspects such as over-

charge and out gassing of lead-acid batteries [11, 22], and performance as a function of temperature [30, 11, 22].

A battery's lifetime is a function of how it operates and the SOC level at the time of use [28, 40, 35, 34, 26, 56]. In Figure 4a, we present three different use profiles: (A), (B), and (C). Regime (A) shows full discharge and charge cycles, (B) depicts short charge and discharge cycles at a high SOC, and (C) depicts short charge and discharge cycles at a low SOC. Given identical charge throughput, life expectancy decreasing by regime is generally: (B), (A), and (C). A cycle counting method would not distinguish between these cases as each small charge and discharge would count as a full cycle. Instead of counting cycles as defined by current reversal, we present an amp-hour (Ah) assessment method (see Figure 4b); that is, we sum the total amount of current (Ah) that passes through the battery for both charge and discharge. The quotient of this value and twice the reference capacity yields the fraction of a cycle completed.

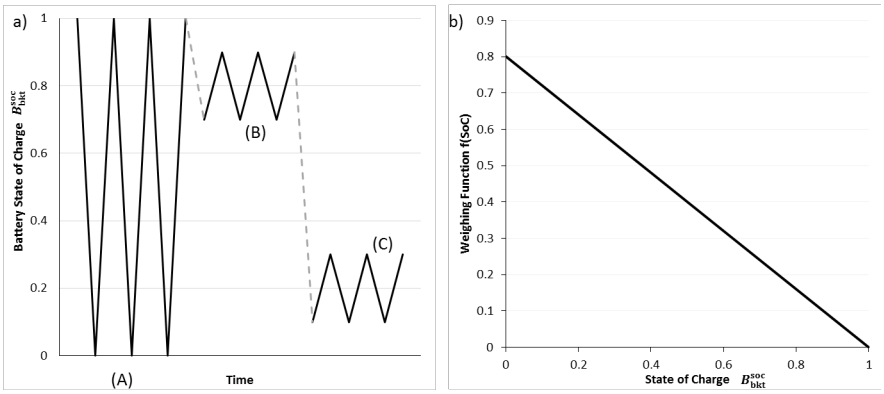

Fig. 4: a) A depth of discharge comparison between three different charge and discharge strategies illustrates the shortcomings of cycle counting. b) A weighting function from which we derive d_b^{soc} and a_b^{soc}, the slope and intercept of the line, respectively, accounts for variable battery aging at different states of charge for an A123 Lithium-ion battery [1].

2.2 Mathematical Formulation

We now present the mathematical formulation of our problem, henceforth referred to as ($\mathcal{P}$). In general, we use lower-case letters for parameters and upper-case letters for variables. We also use lower-case letters for indices and upper-case script letters for sets. Superscripts and accents distinguish between parameters and variables that utilize the same base letter, while subscripts identify elements of a set. Some parameters and variables are only defined for

certain set elements, which are listed in each definition. A plus sign (+) signifies power going into a technology, while a minus sign (−) indicates power leaving. The units of each parameter and variable are provided in brackets after its definition. We use the term "twins" to denote a tuple or a multiple of a certain technology type to distinguish the operational patterns of and, hence, wear on each unit.

Sets

$t \in \mathcal{T}$	set of all time periods [hours]
$j \in \mathcal{J}$	set of all battery and generator technologies
$g \in \mathcal{G} \subset \mathcal{J}$	set of all generator technologies
$b \in \mathcal{B} \subset \mathcal{J}$	set of all battery technologies
$s \in \mathcal{S}$	set of all PV panel types
$k \in \tilde{\mathcal{J}}_j$	set of identical twins of technology j, given by size, type, and manufacturer
$k \in \tilde{\mathcal{G}}_g$	set of all generator twins of type g
$k \in \tilde{\mathcal{B}}_b$	set of all battery twins of type b

Timing Parameters

τ	length of one time period [hours]
ν	ratio of base operation duration to time horizon length [fraction]

Optimization Model Penalty Parameters

$\tilde{c}_j$	cost of procuring one twin of technology type j [$/twin]
c_s	cost of procuring one panel of technology type s [$/panel]
δ_t^f	fuel cost penalty in time period t [$/gal]
ε_j	cycle cost penalty for technology type j [$/(hours, cycles)]

Power System Parameters

d_t^P	steady-state power demand in time period t [W]
$\bar{k}$	overage load coefficient [fraction]
k^s	spinning reserve required relative to PV power [fraction]

Technology Parameters

$\bar{l}_j$	maximum lifetime of technology type j [generator hours, battery cycles]
η_j^+, η_j^-	electric efficiency of power flow into and out of technology type j, respectively [fraction]

$\underline{p}_j, \bar{p}_j$	minimum and maximum power rating, respectively, of technology type j [W]

Generator Parameters

a_g^f, b_g^f, c_g^f	fuel consumption coefficients for generator g $[\frac{gal}{W^2h}, \frac{gal}{Wh}, \frac{gal}{h}]$

PV Parameters

γ_{st}	power output of technology type s in time period t $[\frac{W}{panel}]$
$\bar{n}_s$	maximum allowable number of PV panels of technology type s [panels]

Battery Parameters

a_b^v, b_b^v	battery b linear voltage model slope and intercept coefficients, respectively [V]
d_b^{soc}, a_b^{soc}	battery b linear lifetime model slope and intercept coefficients, respectively [unitless]
b_b^0	battery b state of charge used in initial condition constraints [fraction]
c_b^{ref}	battery b manufacturer-specified capacity [Ah]
c_b^+, c_b^-	battery b charge and discharge capacity rate coefficients, respectively [hours]
r_b^{int}	battery b internal resistance [Ohms]
i_b^{avg}	typical current expected from battery b for both charge and discharge activities [A]
$\underline{s}_b, \bar{s}_b$	battery b state of charge minimum and maximum operational bounds, respectively [fraction]
i_b^{L-}, i_b^{U-}	battery b discharge current lower and upper bound, respectively [A]
i_b^{L+}, i_b^{U+}	battery b charge current lower and upper bound, respectively [A]

where, for our application, the above parameter values are computed as:

$$i_b^{L-} = 0 \quad \forall b \in \mathcal{B}$$
$$i_b^{U-} = \frac{c_b^{ref}}{c_b^- + \tau} \quad \forall b \in \mathcal{B}$$

$$i_b^{L+} = 0 \quad \forall b \in \mathcal{B}$$
$$i_b^{U+} = \frac{c_b^{ref}}{c_b^+} \quad \forall b \in \mathcal{B}$$

Continuous Variables

Power System Variables

L_{jk}	number of expended life cycles for technology type j, twin k [generator hours, battery cycles]
P^{+}_{jkt}, P^{-}_{jkt}	aggregate power into and out of technology type j, twin k in time period t, respectively [W]
P^{PV}_{st}	aggregate power out of PV technology type s in time period t [W]

Generator Variables

$\tilde{F}_t$	amount of fuel used in time period t [gal]

Battery Variables

B^{soc}_{bkt}	state of charge of battery type b, twin k in time period t [fraction]
I^{+}_{bkt}, I^{-}_{bkt}	battery b, twin k current for charge and discharge, respectively, in time period t [A]
V^{soc}_{bkt}	battery b, twin k voltage in time period t [V]

Binary and Integer Variables

Power System Procurement Variables

W_{jk}	1 if technology j, twin k is procured, 0 otherwise
X_s	integer number of PV panels of technology type s procured [panels]

Generator Variables

G_{gkt}	1 if technology type g, twin k is operating in time period t, 0 otherwise

Battery Variables

B^{+}_{bkt}	1 if battery type b, twin k is charging in time period t, 0 otherwise
B^{-}_{bkt}	1 if battery type b, twin k is discharging in time period t, 0 otherwise

Problem ($\mathcal{P}$)
(see §2.3.1 Objective Function)

Minimize

$$\sum_{j\in\mathcal{J}}\sum_{k\in\tilde{\mathcal{J}}_j}\tilde{c}_j W_{jk}+\sum_{s\in\mathcal{S}}c_s X_s+\nu\left(\sum_{j\in\mathcal{J}}\sum_{k\in\tilde{\mathcal{J}}_j}\varepsilon_j L_{jk}+\sum_{t\in\mathcal{T}}\delta_t^f\tilde{F}_t\right) \tag{1}$$

subject to

(see §2.3.2 System Operations)

$$\sum_{j\in\mathcal{J}}\sum_{k\in\tilde{\mathcal{J}}_j}\eta_j^- P_{jkt}^- - \sum_{b\in\mathcal{B}}\sum_{k\in\tilde{\mathcal{B}}_b}P_{bkt}^+ + \sum_{s\in\mathcal{S}}P_{st}^{PV}\geq(1+\bar{k})d_t^P\ \forall t\in\mathcal{T} \tag{2a}$$

$$\sum_{b\in\mathcal{B}}\sum_{k\in\tilde{\mathcal{B}}_b}\eta_b^-\bar{p}_b B_{bkt}^{soc}+\sum_{g\in\mathcal{G}}\sum_{k\in\tilde{\mathcal{G}}_g}\left(\bar{p}_g G_{gkt}-P_{gkt}^-\right)\geq k^s\sum_{s\in\mathcal{S}}P_{st}^{PV}\quad\forall t\in\mathcal{T} \tag{2b}$$

$$W_{j,k-1}\geq W_{jk}\ \ \forall j\in\mathcal{J},k\in\tilde{\mathcal{J}}_j:k>1 \tag{2c}$$

(see §2.3.3 Generator Operations)

$$\underline{p}_g G_{gkt}\leq P_{gkt}^-\leq\bar{p}_g G_{gkt}\quad\forall g\in\mathcal{G},k\in\tilde{\mathcal{G}}_g,t\in\mathcal{T} \tag{3a}$$

$$\tilde{F}_t\geq\tau\sum_{g\in\mathcal{G}}\sum_{k\in\tilde{\mathcal{G}}_g}(a_g^f(P_{gkt}^-)^2+b_g^f P_{gkt}^-+c_g^f G_{gkt})\quad\forall t\in\mathcal{T} \tag{3b}$$

$$G_{gkt}\leq W_{gk}\quad\forall g\in\mathcal{G},k\in\tilde{\mathcal{G}}_g,t\in\mathcal{T} \tag{3c}$$

$$G_{g,k-1,t}\leq G_{gkt}\quad\forall g\in\mathcal{G},k\in\tilde{\mathcal{G}}_g,t\in\mathcal{T}:k>1 \tag{3d}$$

$$P_{g,k-1,t}^-\leq P_{gkt}^-\quad\forall g\in\mathcal{G},k\in\tilde{\mathcal{G}}_g,t\in\mathcal{T}:k>1 \tag{3e}$$

(see §2.3.4 PV Operations)

$$P_{st}^{PV}\leq\gamma_{st}X_s\quad\forall s\in\mathcal{S},t\in\mathcal{T} \tag{4a}$$

$$X_s\leq\bar{n}_s\quad\forall s\in\mathcal{S} \tag{4b}$$

(see§ 2.3.5 Battery Storage Operations)

$$P_{bkt}^+=V_{bkt}^{soc}I_{bkt}^+\quad\forall b\in\mathcal{B},k\in\tilde{\mathcal{B}}_b,t\in\mathcal{T} \tag{5a}$$

$$P_{bkt}^-=V_{bkt}^{soc}I_{bkt}^-\quad\forall b\in\mathcal{B},k\in\tilde{\mathcal{B}}_b,t\in\mathcal{T} \tag{5b}$$

$$B^{soc}_{bkt} = B^{soc}_{bk,t-1} + \frac{\tau(\eta^+_b I^+_{bkt} - I^-_{bkt})}{c^{ref}_b} \quad \forall b \in \mathcal{B}, k \in \tilde{\mathcal{B}}_b, t \in \mathcal{T} : t > 1 \tag{5c}$$

$$\underline{s}_b W_{bk} \leq B^{soc}_{bkt} \leq \bar{s}_b W_{bk} \quad \forall b \in \mathcal{B}, k \in \tilde{\mathcal{B}}_b, t \in \mathcal{T} \tag{5d}$$

$$B^{soc}_{bkt} \leq B^{soc}_{b,k-1,t} + (1 - W_{bk}) \quad \forall b \in \mathcal{B}, k \in \tilde{\mathcal{B}}_b, t \in \mathcal{T} : k > 1 \tag{5e}$$

$$B^{soc}_{bkt} \geq B^{soc}_{b,k-1,t} - (1 - W_{bk}) \quad \forall b \in \mathcal{B}, k \in \tilde{\mathcal{B}}_b, t \in \mathcal{T} : k > 1 \tag{5f}$$

$$V^{soc}_{bkt} = a^v_b B^{soc}_{bk,t-1} + b^v_b (B^+_{bkt} + B^-_{bkt}) + i^{avg}_b r^{int}_b (B^+_{bkt} - B^-_{bkt}) \quad \forall b \in \mathcal{B}, k \in \tilde{\mathcal{B}}_b, t \in \mathcal{T} : t > 1 \tag{5g}$$

$$\underline{p}_b B^-_{bkt} \leq P^-_{bkt} \leq \bar{p}_b B^-_{bkt} \; \forall b \in \mathcal{B}, k \in \tilde{\mathcal{B}}_b, t \in \mathcal{T} \tag{5h}$$

$$\underline{p}_b B^+_{bkt} \leq P^+_{bkt} \leq \bar{p}_b B^+_{bkt} \; \forall b \in \mathcal{B}, k \in \tilde{\mathcal{B}}_b, t \in \mathcal{T} \tag{5i}$$

$$I^-_{bkt} \leq i^{U-}_b B^{soc}_{bk,t-1} \quad \forall b \in \mathcal{B}, k \in \tilde{\mathcal{B}}_b, t \in \mathcal{T} : t > 1 \tag{5j}$$

$$i^{L-}_b B^-_{bkt} \leq I^-_{bkt} \leq i^{U-}_b B^-_{bkt} \quad \forall b \in \mathcal{B}, k \in \tilde{\mathcal{B}}_b, t \in \mathcal{T} \tag{5k}$$

$$i^{L+}_b B^+_{bkt} \leq I^+_{bkt} \leq i^{U+}_b B^+_{bkt} \quad \forall b \in \mathcal{B}, k \in \tilde{\mathcal{B}}_b, t \in \mathcal{T} \tag{5l}$$

$$B^+_{bkt} + B^-_{bkt} \leq W_{bk} \quad \forall b \in \mathcal{B}, k \in \tilde{\mathcal{B}}_b, t \in \mathcal{T} \tag{5m}$$

$$B^+_{bkt} + B^-_{b'k't} \leq 1 \quad \forall b, b' \in \mathcal{B}; k, k' \in \tilde{\mathcal{B}}_b; t \in \mathcal{T} : b \neq b', k \neq k' \tag{5n}$$

(see §2.3.6 Lifecycle)

$$L_{gk} \geq \tau \sum_{t \in \mathcal{T}} G_{gkt} \quad \forall g \in \mathcal{G}, k \in \tilde{\mathcal{G}}_g \tag{6a}$$

$$L_{bk} \geq \tau \sum_{t \geq 2} \left(\frac{I^+_{bkt} + I^-_{bkt}}{2c^{ref}_b} \right) (a^{soc}_b - d^{soc}_b B^{soc}_{bk,t-1}) \quad \forall b \in \mathcal{B}, k \in \hat{\mathcal{B}}_b \tag{6b}$$

$$L_{jk} \leq \frac{\bar{l}_j}{\nu} W_{jk} \quad \forall j \in \mathcal{J}, k \in \tilde{\mathcal{J}}_j \tag{6c}$$

(see §2.3.7 Non-negativity and Integrality)

$$P^{-}_{jkt}, P^{+}_{jkt} \geq 0 \quad \forall j \in \mathcal{J}, k \in \tilde{\mathcal{J}}_j, t \in \mathcal{T} \tag{7a}$$

$$L_{jk} \geq 0 \quad \forall j \in \mathcal{J}, k \in \tilde{\mathcal{J}}_j \tag{7b}$$

$$\tilde{F}_t \geq 0 \quad t \in \mathcal{T} \tag{7c}$$

$$P^{PV}_{st} \geq 0 \quad \forall s \in \mathcal{S}, t \in \mathcal{T} \tag{7d}$$

$$B^{soc}_{bkt}, I^{+}_{bkt}, I^{-}_{bkt}, V^{soc}_{bkt} \geq 0 \quad \forall b \in \mathcal{B}, k \in \tilde{\mathcal{B}}_b, t \in \mathcal{T} \tag{7e}$$

$$X_s \geq 0 \quad \text{integer} \quad \forall s \in \mathcal{S} \tag{7f}$$

$$W_{jk} \quad \text{binary} \quad \forall j \in \mathcal{J}, k \in \tilde{\mathcal{J}}_j \tag{7g}$$

$$G_{gkt} \quad \text{binary} \quad \forall g \in \mathcal{G}, k \in \tilde{\mathcal{G}}_g, t \in \mathcal{T} \tag{7h}$$

$$B^{+}_{bkt}, B^{-}_{bkt} \quad \text{binary} \quad \forall b \in \mathcal{B}, k \in \tilde{\mathcal{B}}_b, t \in \mathcal{T} \tag{7i}$$

2.3 Detailed Discussion of Formulation

We model the optimal design and dispatch problem as a nonconvex, mixed-integer, nonlinear program. Instances of this problem are challenging to solve, because of the nonconvex relationships between variables, and the lengthy time horizon, i.e., annual with hourly fidelity. The presence of battery state-of-charge relationships and of battery lifecycle constraints implies that the model does not decompose readily by time step. Below, we comment on each of these characteristics of our model in turn before we suggest procedures to expedite solutions.

2.3.1 Objective Function

The objective function (1), minimizes the sum of four terms: (i) the cost associated with procuring various battery and generator technologies; (ii) the cost associated with procuring various PV panels; (iii) an arbitrarily weighted measure of the life cycles used by each technology over the total length of operation; and (iv) a weighted measure of the cost of fuel. Our application pertains to forward operating bases with a maximum lifetime of one year. To reconcile time horizon lengths of other than a year, we apply the parameter ν, which adjusts operational costs accordingly.

2.3.2 System Operations

Constraint (2a) ensures that the hourly dispatch strategy meets demand. The first term represents the power from the generators and batteries, accounting for power system losses; the second term captures the power to charge the batteries, and the third term reflects the contributions of PV power. The

right-hand side is the product of the forecasted demand for the time period and an overage load factor. Due to the intermittence of solar power, constraint (2b) enforces "spinning reserves," which ensure that a backup power source, either batteries and/or generators, is available to meet a fraction of the load supplied by PV. Constraint (2c) breaks symmetry and forces the procurement of twins of technology j to occur in a fixed order [54]. These constraints do not guarantee a decrease in computation time in every instance we solve, but they do tend to minimize long solution times (see Section 4).

2.3.3 Generator Operations

If a generator is running, constraint (3a) bounds output power between a minimum and maximum manufacturer-specified level. Constraint (3b) determines the amount of fuel used during time period t, which, if $a_g^f = 0$, is linear. Constraint (3c) connects procurement to dispatch. Constraints (3d) and (3e) prioritize the use of technology twins to reduce symmetry [54]. These constraints force the dispatch of generators in lexicographic order, which produces unequal wear and is therefore contrary to their likely dispatch method; in a real dispatch situation, an equal-wear strategy could be pursued without compromising the objective function value.

2.3.4 PV Operations

We limit the PV output power per panel to γ_{st} in constraint (4a). The anticipated solar panel output results from a PVWatts simulation run a priori, which accounts for performance characteristics such as location, panel efficiency, tilt, and angle. Constraint (4b) limits the number of panels considered for procurement given the expected land area available.

2.3.5 Battery Storage Operations

Constraints (5a) and (5b) represent the nonlinear relationship between voltage, current, and the power associated with charging and discharging the battery, respectively. Constraint (5c) updates the battery SOC, which is a function of its previous SOC and the discharge and charge currents. An efficiency parameter associated with the second term signifies that when the battery charges, the state of charge receives a fraction of the incoming power due to the conversion from AC to DC power. For time period $t = 1$, the constraint is:

$$B_{bkt}^{soc} = b_b^0 W_{bk} + \tau \left(\frac{\eta_b^+ I_{bkt}^+ - I_{bkt}^-}{c_b^{ref}} \right) \quad \forall b \in \mathcal{B}, k \in \tilde{\mathcal{B}}_b, t = 1 \tag{8}$$

Constraint (5d) bounds the SOC of a battery to a minimum and maximum level. Constraints (5e) and (5f) ensure that the batteries operate in droop, rather than individually, to avoid the situation in which one battery is used to charge another. When considering only one battery for procurement, these

constraints are redundant and may be removed. Constraint (5g) models the battery voltage as a function of its previous state of charge and the direction of current flow, which, for state of charge levels between a certain range, is linear (see Figure 3a).

Constraints (5h) and (5i) bound the net power flow of each battery per time period, while constraints (5j) through (5l) similarly constrain current flow. For time period $t = 1$, constraint (5j) is:

$$I^{-}_{bkt} \leq i^{U-}_{b} b^{0}_{b} B^{-}_{bkt} \quad \forall b \in \mathcal{B}, k \in \tilde{\mathcal{B}}_b, t = 1 \tag{9}$$

Constraints (5m) and (5n) prevent simultaneous charge and discharge for a given battery, and for different battery-twin combinations, respectively.

2.3.6 Lifecycle

Constraint (6a) counts the number of operational hours of a generator. Constraint (6b) counts weighted equivalent cycles for batteries. A battery's lifecycle is a function of both the amount of the charge and discharge currents as well as the SOC level at which the charge or discharge occurs. Because the lifecycle constraint considers both charge and discharge, i.e., two opposite-direction-operations to which together we refer as a round trip, we divide by two. Constraint (6c) limits technology lifetime.

2.3.7 Non-negativity and Integrality

Finally, constraints (7a) - (7e) ensure that the appropriate variables in our formulation assume continuous, non-negative values. Constraints (7f) - (7i) enforce integer and binary restrictions, as appropriate.

2.4 Linearization

Model ($\mathcal{P}$) is nonlinear in that there is one quadratic term (see constraint (3b)), and bilinear terms exist within constraints (5a), (5b), and (6b). To increase tractability of the corresponding model instances, we present ($\mathcal{U}$), a linearization of ($\mathcal{P}$) which corresponds to an under-estimation of the original problem.

We can approximate a quadratic function by using piecewise linear functions; however, in our case, the data provided by the manufacturers corresponds to a line (see Figure 2), so we set a^{f}_{g} equal to 0, thereby eliminating the quadratic term. The bilinear terms assume one of two forms: (i) the product of a binary variable and a continuous variable, and (ii) the product of two continuous variables. We provide an exact method to linearize the former, and use a convex under-estimation technique for the latter. We do not explicitly

present the constraints for the case in which $t = 1$ because the only difference is that for this case, b_b^0 replaces $B_{bk,t-1}^{soc}$ (which occurs when $t > 1$).

Substituting the voltage constraint (5g) directly into the power constraints (5a) and (5b), we obtain:

$$P_{bkt}^{+} = \left(a_b^v B_{bk,t-1}^{soc} + b_b^v (B_{bkt}^{+} + B_{bkt}^{-}) + i_b^{avg} r_b^{int} (B_{bkt}^{+} - B_{bkt}^{-}) \right) I_{bkt}^{+} \quad \forall b \in \mathcal{B}, k \in \tilde{\mathcal{B}}_b, t \in \mathcal{T} : t > 1 \tag{10}$$

$$P_{bkt}^{-} = \left(a_b^v B_{bk,t-1}^{soc} + b_b^v (B_{bkt}^{+} + B_{bkt}^{-}) + i_b^{avg} r_b^{int} (B_{bkt}^{+} - B_{bkt}^{-}) \right) I_{bkt}^{-} \quad \forall b \in \mathcal{B}, k \in \tilde{\mathcal{B}}_b, t \in \mathcal{T} : t > 1 \tag{11}$$

We can simplify equations (10) and (11) by distributing the respective current variable and removing the irrelevant charge or discharge binary variable in each equation. For example, if a battery is charging during a time period, it cannot be discharging, so we remove the discharge binary variables B_{bkt}^{-}.

$$P_{bkt}^{+} = a_b^v B_{bk,t-1}^{soc} I_{bkt}^{+} + (b_b^v + i_b^{avg} r_b^{int}) B_{bkt}^{+} I_{bkt}^{+} \quad \forall b \in \mathcal{B}, k \in \tilde{\mathcal{B}}_b, t \in \mathcal{T} : t > 1 \tag{12}$$

$$P_{bkt}^{-} = a_b^v B_{bk,t-1}^{soc} I_{bkt}^{-} + (b_b^v - i_b^{avg} r_b^{int}) B_{bkt}^{-} I_{bkt}^{-} \quad \forall b \in \mathcal{B}, k \in \tilde{\mathcal{B}}_b, t \in \mathcal{T} : t > 1 \tag{13}$$

We distribute the terms on the right hand side of the lifecycle constraint (6b) to identify bilinear terms consisting of SOC and current:

$$L_{bk} \geq \tau \sum_{t \geq 2} \left(\frac{a_b^{soc} I_{bkt}^{+} - d_b^{soc} B_{bk,t-1}^{soc} I_{bkt}^{+} + a_b^{soc} I_{bkt}^{-} - d_b^{soc} B_{bk,t-1}^{soc} I_{bkt}^{-}}{2 c_b^{ref}} \right) \quad \forall b \in \mathcal{B}, k \in \hat{\mathcal{B}}_b \tag{14}$$

Auxiliary Variables

Equations (12), (13), and (14) contain two sets of bi-linear terms, for each of which we define a nonnegative continuous variable:

Y_{bkt}^{+}, Y_{bkt}^{-}	battery b, twin k exact linearization variable representing the product of a binary and continuous variable for charge and discharge, respectively, in time period t [A]
Z_{bkt}^{+}, Z_{bkt}^{-}	battery b, twin k linear approximation variable representing the product of two continuous variables for charge and discharge, respectively, in time period t [A]

$$Y^+_{bkt}, Y^-_{bkt}, Z^+_{bkt}, Z^-_{bkt} \geq 0 \quad \forall b \in \mathcal{B}, k \in \tilde{\mathcal{B}}_b, t \in \mathcal{T} \tag{15}$$

$$Y^+_{bkt} = B^+_{bkt} I^+_{bkt} \quad \forall b \in \mathcal{B}, k \in \tilde{\mathcal{B}}_b, t \in \mathcal{T} \tag{16}$$
$$Y^-_{bkt} = B^-_{bkt} I^-_{bkt} \quad \forall b \in \mathcal{B}, k \in \tilde{\mathcal{B}}_b, t \in \mathcal{T} \tag{17}$$

$$Z^+_{bkt} = B^{soc}_{bk,t-1} I^+_{bkt} \quad \forall b \in \mathcal{B}, k \in \tilde{\mathcal{B}}_b, t \in \mathcal{T} : t > 1 \tag{18}$$
$$Z^-_{bkt} = B^{soc}_{bk,t-1} I^-_{bkt} \quad \forall b \in \mathcal{B}, k \in \tilde{\mathcal{B}}_b, t \in \mathcal{T} : t > 1 \tag{19}$$

We then substitute these variables directly into (12), (13), and (14):

$$P^+_{bkt} = a^v_b Z^+_{bkt} + (b^v_b + i^{avg}_b r^{int}_b) Y^+_{bkt} \quad \forall b \in \mathcal{B}, k \in \tilde{\mathcal{B}}_b, t \in \mathcal{T} \tag{20}$$
$$P^-_{bkt} = a^v_b Z^-_{bkt} + (b^v_b - i^{avg}_b r^{int}_b) Y^-_{bkt} \quad \forall b \in \mathcal{B}, k \in \tilde{\mathcal{B}}_b, t \in \mathcal{T} \tag{21}$$
$$L_{bk} \geq \tau \sum_{t \geq 2} \left(\frac{a^{soc}_b I^+_{bkt} - d^{soc}_b Z^+_{bkt} + a^{soc}_b I^-_{bkt} - d^{soc}_b Z^-_{bkt}}{2 c^{ref}_b} \right) \quad \forall b \in \mathcal{B}, k \in \tilde{\mathcal{B}}_b \tag{22}$$

Constraint (6b) presents a symmetric function that penalizes both charge and discharge operations equally as a fraction of capacity. Given our definition of SOC per constraint (5c), which implies the battery needs to charge in order to discharge, we can simplify constraint (22) by multiplying it by two, which cancels the 2 in the denominator, and by removing either the charge or discharge variables. We choose to remove the discharge variables because our approximation for Z^+_{bkt} is more accurate (see Table 10).

$$L_{bk} \geq \tau \sum_{t \geq 2} \left(\frac{a^{soc}_b I^+_{bkt} - d^{soc}_b Z^+_{bkt}}{c^{ref}_b} \right) \quad \forall b \in \mathcal{B}, k \in \tilde{\mathcal{B}}_b \tag{23}$$

All constraints involving bilinear terms contain Y^+_{bkt}, Y^-_{bkt}, Z^+_{bkt}, and/or Z^-_{bkt}. We execute an exact technique to linearize the bilinearities associated with Y^+_{bkt} and Y^-_{bkt}; we invoke an approximation to eliminate the nonlinearities associated with Z^+_{bkt} and Z^-_{bkt}.

2.4.1 Exact Linearization

We apply the operational bounds of charge and discharge current to Y^+_{bkt} and Y^-_{bkt}, respectively:

$$i^{L+}_b B^+_{bkt} \leq Y^+_{bkt} \leq i^{U+}_b B^+_{bkt} \quad \forall b \in \mathcal{B}, k \in \tilde{\mathcal{B}}_b, t \in \mathcal{T} \tag{24a}$$
$$i^{L-}_b B^-_{bkt} \leq Y^-_{bkt} \leq i^{U-}_b B^-_{bkt} \quad \forall b \in \mathcal{B}, k \in \tilde{\mathcal{B}}_b, t \in \mathcal{T} \tag{24b}$$

We can further constrain Y^-_{bkt} by the upper bound on the battery's discharge current and the SOC, because $B^{soc}_{bkt} \leq B^-_{bkt}$ $\forall b \in \mathcal{B}, k \in \tilde{\mathcal{B}}_b, t \in \mathcal{T}$ when the battery is discharging, i.e., $B^-_{bkt} = 1$; this tightens the upper bound imposed by constraint (24b). If the battery is not discharging, then $B^-_{bkt} = 0$, which forces $Y^-_{bkt} = 0$.

$$Y^-_{bkt} \leq i^{U-}_b B^{soc}_{bk,t-1} \quad \forall b \in \mathcal{B}, k \in \tilde{\mathcal{B}}_b, t \in \mathcal{T} : t > 1 \tag{24c}$$

Note that constraint (24c) is similar to (5j). We do not further constrain Y^+_{bkt} because, for the parameters in our application, i.e., i^{U+}_b, the bound is sufficiently tight.

We then relate Y^+_{bkt} and Y^-_{bkt} to the respective current variable using an exact relationship. For example, when a battery charges, B^+_{bkt} is 1, which implies that $I^+_{bkt} = Y^+_{bkt}$. If B^+_{bkt} is 0, Y^+_{bkt} is 0 by (24a), and $-i^{U+}_b \leq I^+_{bkt} \leq i^{U+}_b$ (which is redundant). The same logic holds for the discharge case.

$$-i^{U+}_b(1 - B^+_{bkt}) \leq I^+_{bkt} - Y^+_{bkt} \leq i^{U+}_b(1 - B^+_{bkt}) \quad \forall b \in \mathcal{B}, k \in \tilde{\mathcal{B}}_b, t \in \mathcal{T} \tag{24d}$$
$$-i^{U-}_b(1 - B^-_{bkt}) \leq I^-_{bkt} - Y^-_{bkt} \leq i^{U-}_b(1 - B^-_{bkt}) \quad \forall b \in \mathcal{B}, k \in \tilde{\mathcal{B}}_b, t \in \mathcal{T} \tag{24e}$$

By substituting constraints (24a) through (24e) for constraints (16) and (17) and adding nonnegativity of Y^+_{bkt}, Y^-_{bkt}, we achieve an exact reformulation of the product of a binary and continuous variable.

2.4.2 Approximate Linearization

Z^+_{bkt} and Z^-_{bkt} represent the product of two continuous variables, which is both a nonlinear and nonconvex relationship; however, [42] and [12] provide an approximation technique using the convex envelope of the terms comprising the bilinear relationship to obtain a lower bound. We depict this linearization in constraints (25a) through (25h), which replace constraints (18) and (19) in our reformulation.

$$Z^+_{bkt} \geq i^{U+}_b B^{soc}_{bk,t-1} + \bar{s}_b I^+_{bkt} - \bar{s}_b i^{U+}_b \quad \forall b \in \mathcal{B}, k \in \tilde{\mathcal{B}}_b, t \in \mathcal{T} : t > 1 \tag{25a}$$
$$Z^+_{bkt} \geq i^{L+}_b B^{soc}_{bk,t-1} + \underline{s}_b I^+_{bkt} - \underline{s}_b i^{L+}_b \quad \forall b \in \mathcal{B}, k \in \tilde{\mathcal{B}}_b, t \in \mathcal{T} : t > 1 \tag{25b}$$
$$Z^+_{bkt} \leq i^{U+}_b B^{soc}_{bk,t-1} + \underline{s}_b I^+_{bkt} - \underline{s}_b i^{U+}_b \quad \forall b \in \mathcal{B}, k \in \tilde{\mathcal{B}}_b, t \in \mathcal{T} : t > 1 \tag{25c}$$
$$Z^+_{bkt} \leq i^{L+}_b B^{soc}_{bk,t-1} + \bar{s}_b I^+_{bkt} - \bar{s}_b i^{L+}_b \quad \forall b \in \mathcal{B}, k \in \tilde{\mathcal{B}}_b, t \in \mathcal{T} : t > 1 \tag{25d}$$

$$Z^-_{bkt} \geq i^{U-}_b B^{soc}_{bk,t-1} + \bar{s}_b I^-_{bkt} - \bar{s}_b i^{U-}_b \quad \forall b \in \mathcal{B}, k \in \tilde{\mathcal{B}}_b, t \in \mathcal{T} : t > 1 \quad (25e)$$

$$Z^-_{bkt} \geq i^{L-}_b B^{soc}_{bk,t-1} + \underline{s}_b I^-_{bkt} - \underline{s}_b i^{L-}_b \quad \forall b \in \mathcal{B}, k \in \tilde{\mathcal{B}}_b, t \in \mathcal{T} : t > 1 \quad (25f)$$

$$Z^-_{bkt} \leq i^{U-}_b B^{soc}_{bk,t-1} + \underline{s}_b I^-_{bkt} - \underline{s}_b i^{U-}_b \quad \forall b \in \mathcal{B}, k \in \tilde{\mathcal{B}}_b, t \in \mathcal{T} : t > 1 \quad (25g)$$

$$Z^-_{bkt} \leq i^{L-}_b B^{soc}_{bk,t-1} + \bar{s}_b I^-_{bkt} - \bar{s}_b i^{L-}_b \quad \forall b \in \mathcal{B}, k \in \tilde{\mathcal{B}}_b, t \in \mathcal{T} : t > 1 \quad (25h)$$

Thus, $(\mathcal{U})$ removes constraints (5a), (5b), (5g), and (6b) and replaces them with constraints (20) through (25h), and adds a non-negativity constraint (15). The quality of solutions from $(\mathcal{U})$, compared to $(\mathcal{P})$, is directly related to the tightness of the convexified bounds for Z^+_{bkt} and Z^-_{bkt} (see Section 4.4), which are a function of $\underline{s}_b$, $\bar{s}_b$, i^{L+}_b, i^{U+}_b, i^{L-}_b, and i^{U-}_b and originate from the rate-capacity effect of the battery (see constraints (5j) through (5l)).

3 Heuristics

We present a heuristic $\mathcal{H}$ that produces an initial feasible solution to models $(\mathcal{U})$ and $(\mathcal{P})$ quickly by: (i) limiting the set of candidate designs for instances, and (ii) using the better of two myopic dispatch strategies. The heuristic $\mathcal{H}$ possesses the following benefits:

- reduces solution time by eliminating dominated design decisions from the feasible region;
- supplies a branch-and-bound solver with an initial feasible solution, known as a "warm start," which can reduce computation time if the initial solution is close to optimal; and,
- provides a dispatch strategy that is easier to implement in a microgrid controller than following ideal dispatch decisions from model $(\mathcal{U})$, as the solution does not look ahead to future time periods and is feasible for the nonlinear model $(\mathcal{P})$.

That is, not only can we mitigate the unpredictable performance issues associated with mixed-integer (nonlinear) programs by using a fast strategy to produce an initial solution, but we can also demonstrate that such a solution, while not having clairvoyance regarding the demand in future time periods, still yields a near-optimal objective function value.

3.1 Technology Selection

To reduce the size of the problem, we limit generator technologies and number of twins, i.e., the cardinality of sets $\tilde{\mathcal{G}}_g$, using Algorithm 1. Similarly, we limit the number of battery technologies, i.e., the cardinality of $\tilde{\mathcal{B}}_b$, using Algorithm 2. We fix the cardinality of the sets of generators rated less than

100kW to two generators total. We justify our algorithms by the following Pareto analysis of the objective function terms. Specifically, a solution with fewer higher-rated generators dominates a solution with more lower-rated generators, because: (i) the cost of generators per rated power is not linear, e.g., a 15kW generator costs nearly 70% of a 100kW generator (see Table 2); (ii) the objective function penalizes a dispatch strategy that employs a higher number of technologies to meet demand; and (iii) fuel consumption of generators is similar for the four we consider (see Figure 2) regardless of the percent loading at which we operate them.

Algorithm 1 Determines the generator technologies and respective number of twins, i.e., cardinality of $\tilde{\mathcal{G}}_g = \{g1, g2, g3, g4\}$, per instance: see Table 2 for details.

procedure GENERATORTECHS&TWINS
  $MaxDemand \leftarrow \max_{t \in \mathcal{T}} d_t^P$
  if $\frac{MaxDemand}{\bar{P}_{g_1}} \geq 0.9$ **then**
    $|\tilde{\mathcal{G}}_{g_1}| \leftarrow \max\left(1, \lfloor \frac{MaxDemand}{\bar{P}_{g_1}} \rfloor\right)$
    $|\tilde{\mathcal{G}}_{g_2}| \leftarrow 2$
    $|\tilde{\mathcal{G}}_{g_3}| \leftarrow 2$
    $|\tilde{\mathcal{G}}_{g_4}| \leftarrow 2$
  else
    $|\tilde{\mathcal{G}}_{g_1}| \leftarrow 0$
    $|\tilde{\mathcal{G}}_{g_2}| \leftarrow 1$
    $|\tilde{\mathcal{G}}_{g_3}| \leftarrow 1$
    $|\tilde{\mathcal{G}}_{g_4}| \leftarrow 1$

We limit battery procurement to one, but consider up to three sizes per instance based on peak demand (see Figure 6) and Algorithm 2. Thus, for an instance with a maximum demand of 239kW, we would consider battery sizes of 200kW, 150kW, and 100kW.

Algorithm 2 Determines the battery technologies considered, i.e., cardinality of $\tilde{\mathcal{B}}_b = \{b1, b2, b3, b4, b5, b6\}$ per instance: see Table 3 for details.

procedure BATTERYTECHS
  $MaxDemand \leftarrow \max_{t \in \mathcal{T}} d_t^P$
  if $MaxDemand \geq 100kW$ **then**
    for `n` $\in$ `{1,...,4}` **do**
      if MaxDemand $\geq 300kW - 50n$ **then**
        $|\tilde{\mathcal{B}}_{b_n}| \leftarrow 1$
        $|\tilde{\mathcal{B}}_{b_{1+n}}| \leftarrow 1$
        $|\tilde{\mathcal{B}}_{b_{2+n}}| \leftarrow 1$
  else
    $|\tilde{\mathcal{B}}_{b_5}| \leftarrow 1$
    $|\tilde{\mathcal{B}}_{b_6}| \leftarrow 1$

3.2 Initial Feasible Solution

To produce an initial feasible solution for instances of $(\mathcal{U})$, our heuristic, which we term $\mathcal{H}$, uses technologies chosen by Algorithms 1 and 2. That is, $\mathcal{H}$ chooses the better of two different, myopic dispatch strategies for each possible combination of technologies; we term such a combination a *design decision* and the design and dispatch solution a *design-dispatch pair*. Each design decision incorporates diesel generators, batteries, and PV systems. Both dispatch strategies: (i) attempt to run the diesel generators as close to their rated capacities as possible in order to maximize their operating fuel efficiency and longevity; (ii) use the maximum amount of energy from purchased PV systems in order to reduce the fuel cost of running generators and to maximize the return on the solar panels' fixed cost; and (iii) employ batteries primarily to balance load requirements and to provide spinning reserve. For each time period, both strategies initialize all diesel generators to be off, and incrementally add capacity by exchanging the smallest-sized online generator for the next greater size if it is offline, and turning on the smallest generator if no larger offline generator exists. The first dispatch strategy, which we term $\mathcal{H}^1$, increases diesel generator capacity in this way until load and spinning reserve can be met for that time period. The second strategy, which we term $\mathcal{H}^2$, is identical to $\mathcal{H}^1$, but adds diesel capacity as long as generators can be run at their rated capacities. While the former strategy causes batteries to operate at a lower state of charge, the latter strategy typically operates batteries at a higher state of charge owing to its policy of only adding a generator if its capacity is reached. Neither strategy clearly dominates the other for our instances, and neither requires more than a few seconds of computational effort to produce a solution under our implementation. After enumerating all design decisions and subsequently executing $\mathcal{H}^1$ and $\mathcal{H}^2$ on all such decisions, $\mathcal{H}$ chooses the lowest-cost option as the initial solution to $(\mathcal{U})$. Figure 5 provides a flowchart for heuristic $\mathcal{H}^1$; the figure for $\mathcal{H}^2$ is similar. Algorithm 3, given in the Appendix, provides pseudocode for $\mathcal{H}^1$; the pseudocode for $\mathcal{H}^2$ is similar.

4 Numerical Results

We solve instances of $(\mathcal{P})$ as a MINLP and $(\mathcal{U})$ as a MIP on a Sun Fire x2270 m2 with 24 processors (2.93 GHz each), 48 GB RAM, 1 TB HDD, using GAMS 24.1.3 for fourteen different instances, each with specific technological parameter values and system considerations.

4.1 Demand Profile and Technology Information

FOBs (Table 1), which are critical to the Department of Defense's ability to deploy combat forces throughout the world and numbered over 700 during the peak of the Afghanistan and Iraq wars [52], would benefit from hybrid power

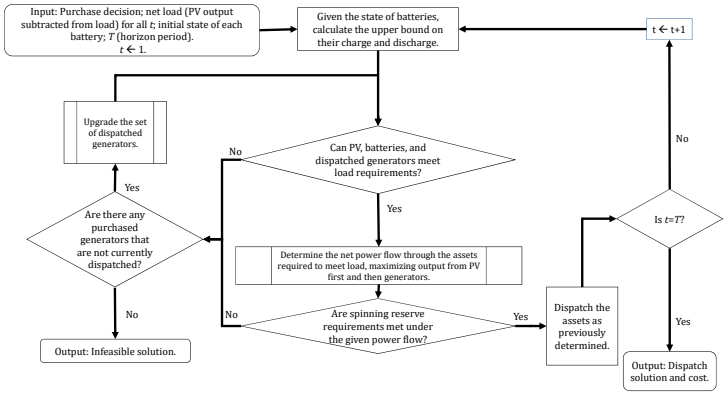

Fig. 5: Heuristic $\mathcal{H}^1$ determines a myopic dispatch strategy for a given design decision.

because currently, power planning is not optimized for efficiency [55]. Military commanders prioritize power reliability over energy efficiency and fuel consumption, which is problematic because resupply operations are dangerous and expensive. In this subsection, we present instance-specific parameters including demand data; technology data, which considers procurement quantities; and a description that details how power flows from the hybrid system to meet demand.

Table 1: We focus our research on remote locations with the characteristics listed in this table.

Characteristic	Requirement
Personnel	<150 People
Land Area ($\bar{n}_s$)	<100m by 100m (flat surface)
Infrastructure Type	<8 tents (20′ by 40′)
Peak Power Demand ($\max d_t^P$)	<300kW
Time Horizon ($\lvert\mathcal{T}\rvert$)	one year ($\lvert\mathcal{T}\rvert$=8,760 hrs)

4.1.1 Demand

We utilize EnergyPlus-simulated [6] FOB demand profiles for fourteen locations throughout the world based on an experiment conducted at the Base Camp Integration Lab (BCIL) at Fort Devens, MA (see Figure 6) [27]. The variation in both the maximum demand and the general shape of the demand profiles provide a robust set for use in testing and validating our models. Within each instance, demand appears to be relatively variable, i.e., there are no discernible, repeating patterns. Because our instances are FOB-specific and

therefore have a lifetime of one-year, ν is equal to one. We set k^s and $\bar{k}$ to 0.3, which is a common fraction used in power planning.

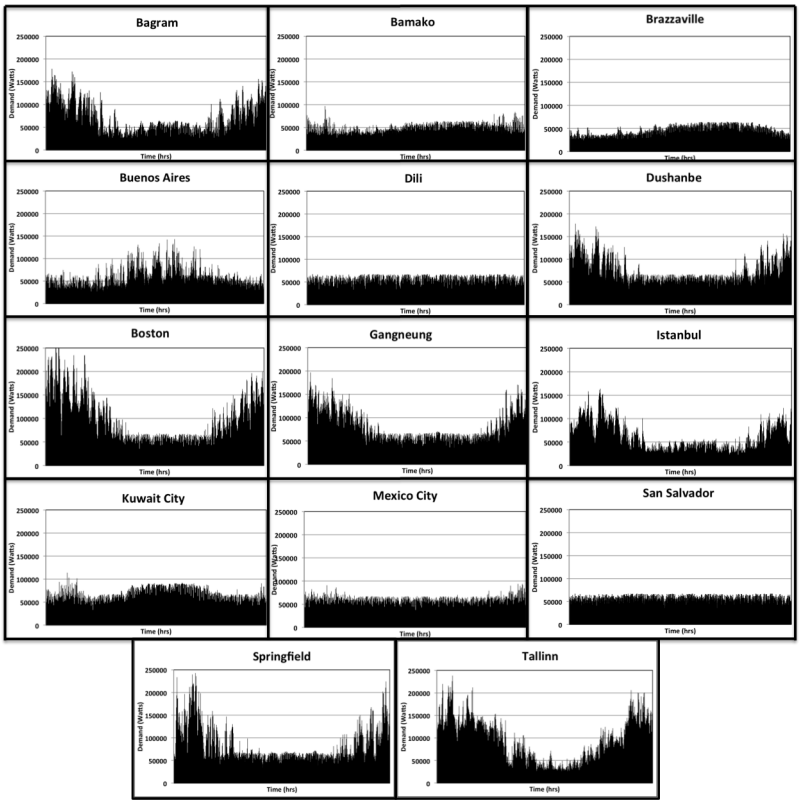

Fig. 6: EnergyPlus simulated year-long ($\nu = 1$) power demand forecasts for fourteen different locations around the world [27] at hourly time fidelity ($\tau = 1$) serve as our set of instances.

4.1.2 Technology and Supply Parameters

The generator technologies we consider are currently in the military's inventory, which implies that the associated maintenance and service parts are as well. There are no hybrid technologies in the military inventory so the PV and battery technologies selected are typical within each of the industries.

Generators

The generators considered in these instances have power ratings ranging from 15kW to 100kW with estimated procurement costs based on a market

analysis of similar technologies. We consider a fully burdened cost of fuel, which is an estimate based on the sum of total cost of all personnel and equipment necessary to move and, when necessary, protect it from the point-of-purchase to point-of-use [52]. We assume an initial fully burdened cost of fuel of $50 per gallon (see Subsection 2.3.1). We do not model the fluctuations in oil price, but assume a small inflation rate. Table 2 displays the characteristics of the generators.

Table 2: Generator technology characteristics used. (See Section 2.2 for definitions and units.)

$g \in \mathcal{G}$	$\bar{p}_g$	$\tilde{c}_g$	ε_g	$\bar{l}_g$	η_g^-	b_g^f	c_g^f
g_1	100,000	$37,691	1	9,000	1	0.0644	0.95
g_2	60,000	$31,967	1	9,000	1	0.0645	0.59
g_3	30,000	$29,376	1	9,000	1	0.0593	0.54
g_4	15,000	$25,573	1	9,000	1	0.0547	0.25

PV

We consider a 1-kW rated mono-crystalline standard PV panel ($4'$ by $6'$) with an 18% efficiency in converting irradiance to power. We limit the number of panels ($\bar{n}_s$) to 75 given spatial restrictions associated with remote hybrid applications. We assume that the procurement cost of each solar panel is $2000, which is equivalent to $2 per Watt. PV panels designed for FOBs need to maintain the expeditionary characteristics of ease of transport and setup so, unlike some PV systems that track the sun, we assume PV panels are fixed-tilt-and-angle panels that rely on a user to erect and position on the appropriate azimuth.

Batteries

We use data from lithium-ion batteries manufactured by A123 [1], which we assume cost $500 per kWh. Battery lifetime parameters result from a linear fit to battery test data from [35]. We scale battery performance parameters to the desired size for stationary applications (see Table 3).

Table 3: Battery technology parameters used. SOC limit $\bar{s}_b$ is 1; $\tau \cdot i_b^{avg} = c_b^{ref}$; all other parameter values are 0. (See Section 2.2 for definitions and units.)

$b \in \mathcal{B}$	$\bar{p}_b$	$\tilde{c}_b$	ε_b	$\bar{l}_b$	η_b^+	η_b^-	r_b^{int}	a_b^v	b_b^v	c_b^{ref}	c_b^-	c_b^+	a_b^{soc}	d_b^{soc}
b_1	250,000	$125,000	1	1,647	0.95	0.95	0.00336	10.62	214.69	1129	0.0401	3	0.801	-0.801
b_2	200,000	$100,000	1	1,647	0.95	0.95	0.0042	10.62	214.69	904	0.0401	3	0.801	-0.801
b_3	150,000	$75,000	1	1,647	0.95	0.95	0.0056	10.62	214.69	678	0.0401	3	0.801	-0.801
b_4	100,000	$50,000	1	1,647	0.95	0.95	0.0084	10.62	214.69	452	0.0401	3	0.801	-0.801
b_5	50,000	$25,000	1	1,647	0.95	0.95	0.01679	10.62	214.69	226	0.0401	3	0.801	-0.801
b_6	25,000	$12,500	1	1,647	0.95	0.95	0.03358	10.62	214.69	113	0.0401	3	0.801	-0.801

Power System

We assume that the hybrid system connects to the power demand through the Power Distribution Illumination System Electrical (PDISE), which has an internal bus capable of system frequency regulation. PDISE is the principal distribution system of the U.S. Army and is compatible with military generator sets from 5kW to 200kW [4, 5, 7]. Preliminary simulation runs have shown our results to be feasible from a power flow standpoint.

Technologies and Twin Decisions

To reduce the size of the problem, we limit generator technologies and number of twins, i.e., the cardinality of sets $\tilde{\mathcal{G}}_g$, using Algorithm 1. Similarly, we limit the number of battery technologies, i.e., the cardinality of $\tilde{\mathcal{B}}_b$, using Algorithim 2. We seed the linear solver with a solution obtained from the heuristics coded in Python 2.7.4 [49] and given in Section 3.

Table 4: Cardinality of sets $\tilde{\mathcal{G}}_g$ and $\tilde{\mathcal{B}}_b$ using Algorithm 1 and Algorithm 2, respectively (see Section 2.2 for definitions).

Instance	$\lvert\tilde{\mathcal{G}}_{g_1}\rvert$	$\lvert\tilde{\mathcal{G}}_{g_2}\rvert$	$\lvert\tilde{\mathcal{G}}_{g_3}\rvert$	$\lvert\tilde{\mathcal{G}}_{g_4}\rvert$	$\lvert\tilde{\mathcal{B}}_{b_1}\rvert$	$\lvert\tilde{\mathcal{B}}_{b_2}\rvert$	$\lvert\tilde{\mathcal{B}}_{b_3}\rvert$	$\lvert\tilde{\mathcal{B}}_{b_4}\rvert$	$\lvert\tilde{\mathcal{B}}_{b_5}\rvert$	$\lvert\tilde{\mathcal{B}}_{b_6}\rvert$
Bagram	2	2	2	2	0	1	1	1	0	0
Bamako	1	2	2	2	0	0	0	1	1	1
Boston	3	2	2	2	1	1	1	0	0	0
Brazzaville	0	1	1	1	0	0	0	0	1	1
Buenos Aires	2	2	2	2	0	0	1	1	1	0
Dili	0	1	1	1	0	0	0	0	1	1
Dushanbe	2	2	2	2	0	1	1	1	0	0
Gangneung	3	2	2	2	0	1	1	1	0	0
Istanbul	2	2	2	2	0	1	1	1	0	0
Kuwait	2	2	2	2	0	0	1	1	1	0
Mexico City	1	2	2	2	0	0	0	1	1	1
San Salvador	0	1	1	1	0	0	0	0	1	1
Springfield	3	2	2	2	1	1	1	0	0	0
Tallinn	3	2	2	2	1	1	1	0	0	0

4.2 Solving ($\mathcal{P}$)

We attempt to solve ($\mathcal{P}$) for a smaller time horizon of 24 hours using existing MINLP solvers at their default settings that accept models coded in GAMS version 24.1.3 [21], which include BARON version 12.5 [50] and Couenne (Couenne Library 0.4) [18], as well as the open-source solver BONMIN (BONMIN Library 1.7) [20]. BONMIN solves a continuous nonlinear program at each node of the search tree, while BARON attempts to underestimate the objective function. Couenne, similarly, uses linear relaxations to bound the

problem. Any feasible solution to ($\mathcal{P}$) provides an upper bound to the problem. We set termination conditions as the minimum of a 5% optimality gap and a time limit of three hours per instance.

Table 5: The size of ($\mathcal{P}$) for a time horizon of one day ($|\mathcal{T}|$=24) over all instances ranges based on the set of technologies. "Maximum" represents the instances that consider the highest number of technologies, while "Minimum" depicts the contrary.

	Constraints		**Variables**	
	Linear	**Nonlinear**	**Continuous**	**Binary**
Maximum	2,145	504	1,176	491
Minimum	834	336	638	198

The nonconvexity of ($\mathcal{P}$) challenges these solvers (Table 6). BARON solves ($\mathcal{P}$) for four of the fourteen instances within the prescribed criteria, while BONMIN solves only two given the same criteria. Interestingly, the former solver provides tighter gaps than the latter, despite the latter being only a local solver and therefore providing only local lower bounds. Couenne yields feasible solutions for all instances, but none within the desired gap. By contrast, when we solve ($\mathcal{U}$) for $|\mathcal{T}| = 24$ hours, we obtain solutions to all fourteen instances within the desired gap in less than one second. Seeding ($\mathcal{P}$) with the procurement decision from ($\mathcal{U}$) and solving with any of the three pieces of nonlinear software we use did not improve performance; seeding the nonlinear model with more than the procurement decision from the linear model renders the constraints associated with battery state-of-charge relationships and battery lifecycle infeasible. The poor performance of these MINLP solvers on the majority of these small instances suggests that ($\mathcal{P}$) is not a tractable formulation; therefore, we instead focus our efforts on ($\mathcal{U}$).

4.3 Solving ($\mathcal{U}$)

Our model ($\mathcal{U}$) is a MIP for which we solve all fourteen instances using CPLEX version 12.5.1.0 [2], a commercial state-of-the-art solver that employs the branch-and-bound algorithm coupled with heuristics to improve the best integer solution and cuts to improve bounds. We also employ our own heuristics (see Section 3), the purpose of which is to provide our linear-integer solver with a "warm start"; however, because they do so in a myopic manner, not having clairvoyance regarding the variability in the load still allows us to produce solutions within approximately 5% of optimality with designs that can be implemented in the field, thus mitigating the potential, detrimental effects on our solution of not having solved a stochastic model.

Because operational decisions at the beginning of the year likely have little impact on those at the end of the year, we attempt to reduce model size

Table 6: Solutions from ($\mathcal{P}$) for each instance given a shortened time horizon ($|\mathcal{T}| = 24$ hrs). Termination criteria: min(3 hours, optimality gap $\leq 5\%$). †Model did not find a feasible solution.

	BARON		BONMIN		Couenne	
Instance	**Gap (%)**	**Time (HR:MIN)**	**Gap (%)**	**Time (HR:MIN)**	**Gap (%)**	**Time (HR:MIN)**
Bagram	5.24	3:00	†	3:00	88.00	3:00
Bamako	8.50	3:00	17.44	3:00	71.52	3:00
Boston	5.86	3:00	†	3:00	85.18	3:00
Brazzaville	0.80	0:42	18.76	3:00	64.93	3:00
Buenos Aires	7.39	3:00	23.57	3:00	66.05	3:00
Dili	11.93	3:00	24.75	3:00	59.54	3:00
Dushanbe	5.11	3:00	†	3:00	86.81	3:00
Gangneung	0.06	0:02	3.44	0:26	83.30	3:00
Istanbul	9.21	3:00	9.99	3:00	70.72	3:00
Kuwait	17.35	3:00	17.35	3:00	69.21	3:00
Mexico City	17.24	3:00	17.24	3:00	67.30	3:00
San Salvador	6.99	3:00	0.00	1:29	63.30	3:00
Springfield	4.76	0:11	11.56	3:00	73.27	3:00
Tallinn	0.29	0:01	†	3:00	79.97	3:00

by aggregating instances into three-hour and twelve-hour time periods for all 14 locations with demand, PV power output per system, and fuel cost by period set to the mean of each time period. However, because these decisions are strongly linked by the design, the aggregated scenarios produce solutions insufficiently robust to handle different operating circumstances at different times of the year. Specifically, these solutions are associated with designs that tend to have less battery capacity when compared to those obtained when solving for hourly dispatch. Optimized dispatch with one-hour time periods uses the battery to balance load while running diesel generators at or near the rated capacity; however, longer time periods limit the battery's maximum rate of charge or discharge over a single time period, which curtails the battery utility overall. Furthermore, the model sees less variability and lower peaks with the aggregated values, which can favor designs with diminished diesel and battery capacity that would be infeasible under problems with hourly time periods. Therefore, we consider all 8,760 hours in our instances, which yields large problems (see Table 7), and an incentive to develop strategies to expedite solutions.

To this end, we use the non-default CPLEX setting "Threads 15" to facilitate concurrent optimization and "MemoryEmphasis 1," which attempts to reduce the memory storage requirements of the problem. We set branching priorities based on complexity in the following, decreasing order: battery procurement and generator procurement by rated power. Similar to ($\mathcal{P}$), we set an optimality gap termination condition of 5%; however, we set the time limit to ten hours, because the year-long time horizon greatly increases the size of the problem compared to ($\mathcal{P}$).

Table 7: Size of ($\mathcal{U}$) for each instance ($|\mathcal{T}|$=8,760).

	Constraints	Variables	
	Linear	**Continuous**	**Binary**
Bagram	1,375,333	499,347	175,214
Bamako	1,340,290	499,346	175,214
Boston	1,778,296	621,995	262,821
Brazzaville	700,806	280,334	70,086
Buenos Aires	1,375,333	499,347	175,214
Dili	700,806	280,334	70,086
Dushanbe	1,375,333	499,347	175,214
Gangneung	1,778,296	621,995	262,821
Istanbul	1,375,333	499,347	175,214
Kuwait	1,375,333	499,347	175,214
Mexico City	1,340,290	499,346	175,214
San Salvador	700,806	280,334	70,086
Springfield	1,778,296	621,995	262,821
Tallinn	1,778,296	621,995	262,821

With the heuristic, we are able to find solutions using model ($\mathcal{U}$) for all instances within a 5% optimality gap in three hours or fewer; results are reported using the symmetry-breaking constraints (3e), (5e), and (5f); while their effect on performance is not uniform, we retain these redundant constraints to minimize long solve times. Table 8 displays solutions and solve times for the fourteen instances with and without a warm start; those with a higher maximum demand take longer to solve because the number of allowable procurement decisions is greater (see Table 4).

Table 8: Solutions from ($\mathcal{U}$) for each instance ($|\mathcal{T}|$ = 8,760 hrs). Termination criteria: min(10 hours, optimality gap $\leq$ 5%) (see Section 2.2 for definitions).

	OBJ Value[1] **($)**	**Fuel Use (gal)**	**Gap (%)**	**Time (hrs:min)**	**Procurement**[2]	**Gen Total**[3] **(kW)**	**Max Demand**[4] **(kW)**	**Heuristic**[5] **(hrs:min)**
Bagram	2,092,916	29,048	4.93	6:31	g_1,g_1,g_2,g_3,g_4,g_4,b_2,s_1	305	240	1:31
Bamako	1,062,946	13,789	5.00	3:01	g_1,g_4,b_4,s_1	115	125	1:55
Boston	3,536,683	56,192	3.34	8:24	g_1,g_1,g_1,g_4,b_3,s_1	315	334	0:11
Brazzaville	1,270,267	17,677	3.28	0:47	g_2,g_4,b_5,s_1	75	84	3:09
Buenos Aires	1,678,616	24,015	4.98	7:27	g_1,g_1,b_3,s_1	200	185	0:10
Dili	1,478,706	22,133	4.89	0:36	g_2,b_5,s_1	60	87	0:17
Dushanbe	2,205,276	31,652	3.53	7:57	g_1,g_2,g_3,g_4,g_4,b_2,s_1	220	231	0:18
Gangneung	2,654,282	40,560	4.97	6:00	g_1,g_1,g_1,b_2,s_1	300	255	0:17
Istanbul	2,243,992	33,530	3.99	5:51	g_1,g_1,g_4,b_2,s_1	215	213	0:17
Kuwait	1,690,109	24,322	4.45	4:10	g_1,g_4,b_3,s_1	115	148	0:17
Mexico City	1,178,090	15,811	4.88	7:40	g_1,g_4,b_4,s_1	115	122	0:39
San Salvador	980,405	12,940	1.95	1:03	g_2,g_4,b_5,s_1	75	87	0:09
Springfield	2,655,202	39,569	2.69	7:50	g_1,g_1,g_2,g_4,b_1,s_1	275	315	0:18
Tallinn	4,047,348	64,557	3.24	6:12	g_1,g_1,g_1,g_4,b_3,s_1	315	309	0:17

[1] **OBJ Value**: represents sum of lifecycle, fuel, and procurement costs; see Expression 1.
[2] **Procurement**: note s_1 represents 75 panels. Common to all instances is the purchase of the maximum number of solar panels.
[3] **Gen Total** represents the sum of the power ratings for all procured generators in kW:

$$\sum_{g \in \mathcal{G}} \sum_{k \in \bar{\mathcal{G}}_g} \bar{p}_g W_{gk}.$$

[4] **Max Demand** is the maximum demand in kW per time period per instance over the year-long time horizon: $\max_{t \in \mathcal{T}} (1 + \bar{k}) d_t^P$ [kW].
[5] **Heuristic** represents computation time to solve ($\mathcal{U}$) with a "warm start."

The procurement decisions, measured by the sum of generator power, rely heavily on the maximum power demand of the instance. When purchased,

solar panels reduce the effective demand, but we limit their procurement due to the large area they occupy. Generally, the restrictions on the number of panels limit the total PV output to a fraction of an instance's peak demand so PV rarely provides more power than demanded, thus increasing the necessity for generators.

Generators operating at less than 30% of their rated power use more fuel and require more maintenance. Our solutions demonstrate that generators operate at close to their rated power whenever possible. Figure 7 depicts the quotient of the total number of hours a generator operates at greater than 30% of its capacity and the total number of hours it operates cumulatively over the time horizon. On average throughout all instances, generators operate at or above 30% of their rated power more than 96% of the time. The model chooses to procure batteries for all cases.

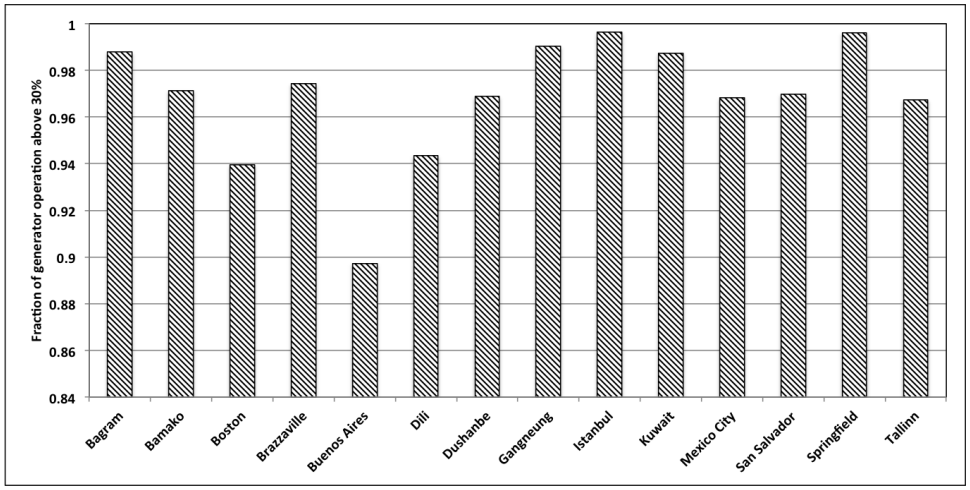

Fig. 7: A graphical representation of generator performance, measured as the quotient of the number of hours a generator operates at greater than 30% rated power and the total number of hours it runs.

Figure 8 is a continuous-time depiction of a discrete 20-hour extract from a year-long dispatch solution to ($\mathcal{U}$) involving two 100kW generators and a 150kW battery. For the battery, positive power values represent discharging, while negative values indicate charging. In Region 1), the demand is greater than 100kW, the maximum rating for the first generator. Instead of turning on the second generator, the model chooses to discharge the battery to meet the load. In Region 2), the load reaches a threshold where the second 100kW generator turns on to meet the demand, but also charges the battery. Lastly, in Region 3), the load drops below the threshold and the second generator turns off while the battery supplies some of the load. This short-term load

shifting allows both generators to operate at high efficiency, which reduces fuel consumption and demonstrates the usefulness of the battery in this situation.

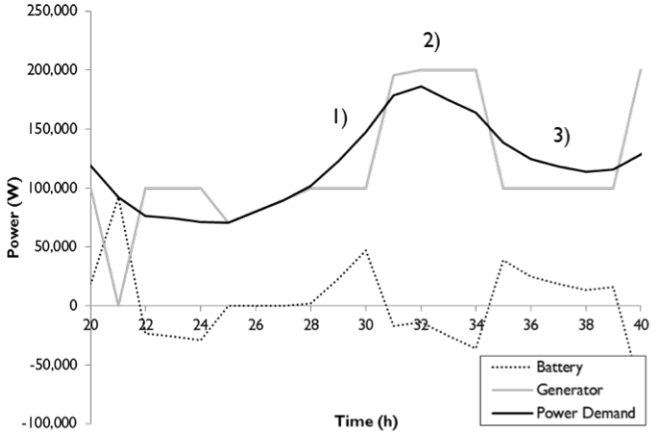

Fig. 8: An example, extracted from the solution to the Buenos Aires instance (see Table 8), of how two 100kW-generators and a battery dispatch power to meet demand for a 20-hour time interval.

Table 9 displays fuel consumption differences between three procurement options solved using ($\mathcal{U}$): (i) hybrid (generator, PV, and battery), (ii) generator-only, and (iii) generator- and PV-only systems. Hybrid systems average 30% fuel savings across all instances compared to a comparably sized generator-only system. In one instance, hybrid systems provide a 50% reduction in fuel use. Although the generator-and-PV-only system is a promising procurement option that also reduces fuel consumption, the addition of the battery further increases fuel savings by nearly 10% across all instances. These savings point to the benefit of employing a method that considers design and dispatch simultaneously. Specifically, were we to consider design in isolation, we would be forced to size the generator capacity for maximum demand to guarantee a feasible solution; PV might not be available to help shave this peak while the battery might not be charged to its maximum capacity. Because fuel use contributes significantly to the objective function value, we could expect design and dispatch solutions optimized in isolation to increase the objective function value correspondingly.

4.4 Solution Quality

In this section, we present an analysis of the quality of solutions from ($\mathcal{U}$) by identifying both where our approximations are imperfect and the magnitude of these errors compared to the nonlinear model ($\mathcal{P}$). We define the following metrics:

Table 9: Fuel consumption results for ($\mathcal{U}$) resulting from three procurement options, which include (i) a hybrid system (generator, PV, and battery), (ii) a generator-only system, and (iii) a generator- and PV-only system, for each instance ($|\mathcal{T}|$ = 8,760 hrs). Termination criteria: min(10 hours, optimality gap ≤ 5%).

	Hybrid System	Generator-Only			Generator & Solar		
	Fuel Consumption (gallons)	Fuel Consumption (gallons)	Fuel Increase vs Hybrid System (gallons)	Fuel Increase / Fuel Consumption	Fuel Consumption (gallons)	Fuel Increase vs. Hybrid System (gallons)	Fuel Increase / Fuel Consumption
Bagram	29,048	43,555	14,507	33%	34,265	5,217	15%
Bamako	13,789	25,623	11,834	46%	17,008	3,219	19%
Boston	56,192	67,484	11,292	17%	58,188	1,996	3%
Brazzaville	17,677	27,405	9,728	35%	19,301	1,624	8%
Buenos Aires	24,015	34,283	10,268	30%	25,974	1,959	8%
Dili	22,133	34,758	12,625	36%	23,353	1,220	5%
Dushanbe	31,652	43,555	11,903	27%	35,508	3,856	11%
Gangneung	40,560	48,939	8,379	17%	42,864	2,304	5%
Istanbul	33,530	42,513	8,983	21%	35,548	2,018	6%
Kuwait	24,322	35,994	11,672	32%	26,268	1,946	7%
Mexico City	15,811	27,231	11,420	42%	18,179	2,368	13%
San Salvador	12,940	26,113	13,173	50%	16,263	3,323	20%
Springfield	39,569	50,934	11,365	22%	42,955	3,386	8%
Tallinn	64,557	70,736	6,179	9%	67,085	2,528	4%

P^+_{bkt}, P^-_{bkt} power into and out of battery b, twin k, in time period t, respectively, computed from a dispatch solution obtained from ($\mathcal{U}$)

$\hat{P}^+_{bkt}, \hat{P}^-_{bkt}$ power computed via nonlinear constraints (12) and (13), respectively, into and out of battery b, twin k, in time period t given values of I^+_{bkt} and I^-_{bkt}, respectively, and $B^{soc}_{bk,t-1}$ obtained from ($\mathcal{U}$)

$\delta^+_{bkt}, \delta^-_{bkt}$ the difference between the actual power into and out of battery b, twin k, in time period t as modeled in ($\mathcal{U}$) (see constraints (20) and (21)), respectively, and the corresponding theoretical power as modeled in ($\mathcal{P}$) [kW]

$\hat{d}^p_{bk}$ the sum over the time horizon of the quotient of the difference between the total amount of battery b, twin k power over-estimated and the total amount underestimated, and the demand converted to [kW] [%]

$\hat{L}_{bk}$ theoretical lifecycles consumed by battery b, twin k over the time horizon, as modeled in ($\mathcal{P}$) per constraint (6b), calculated post run

δ^l_{bk} the quotient of the theoretical and actual lifecycles of battery b, twin k (see constraints (6b) in ($\mathcal{P}$) and (23) in ($\mathcal{U}$), respectively)

$$\delta^-_{bkt} = (P^-_{bkt} - \hat{P}^-_{bkt}) \quad \forall b \in \mathcal{B}, k \in \tilde{\mathcal{B}}_b, t \in \mathcal{T} \tag{26}$$

$$\delta^+_{bkt} = (P^+_{bkt} - \hat{P}^+_{bkt}) \quad \forall b \in \mathcal{B}, k \in \tilde{\mathcal{B}}_b, t \in \mathcal{T} \tag{27}$$

$$\hat{d}^p_{bk} = \sum_{t \in \mathcal{T}} \left(\frac{\delta^+_{bkt} - \delta^-_{bkt}}{d^P_t} \right) 100\% \quad \forall b \in \mathcal{B}, k \in \tilde{\mathcal{B}}_b \tag{28}$$

$$\delta^l_{bk} = \frac{\hat{L}_{bk}}{L_{bk}} 100\% \quad \forall b \in \mathcal{B}, k \in \tilde{\mathcal{B}}_b \tag{29}$$

The results given in Table 10 demonstrate that across all fourteen instances, relative to a corresponding, hypothetical solution from ($\mathcal{P}$): (i) our model over-estimates P^-_{bkt} by as much as 2.8kW per time period, but this is less than 5% of the average demand; (ii) our model under-estimates P^+_{bkt} by as much as 1kW;

and (iii) the combination of (i) and (ii) over the time horizon contributes to less than 0.02% of the total demand summed over the time horizon. It is possible that changes to the dispatch in one time period affect dispatch in subsequent time periods and, hence, the quality of our approximations; however, we seek a dispatch solution at hourly time fidelity, which assumes a steady-state demand and implies that small perturbations due to approximation error are not particularly consequential. Lastly, (iv) our model over-approximates lifecycles consumed by roughly 25%. This is acceptable because lifecycles provide only a small contribution to the objective function value; furthermore, this over-approximation results in a conservative assessment, which is desirable to offset our omission of temperature effects, which may age the battery more rapidly than estimated in a solution to $(\mathcal{U})$.

The approximation error of our model results from the bounds corresponding to the linearization associated with auxiliary variables Z^+_{bkt} and Z^-_{bkt}. Our model seeks to minimize Z^+_{bkt} as a means to conserve power generated either to enter the battery or for direct use in meeting demand. On the other hand, the higher the value of Z^-_{bkt}, the more power we are able to withdraw from the battery. The tightness of the coefficients on the variables on the right hand side of constraints (25a) and (25b) in the case of Z^+_{bkt}, and of constraints (25g) and (25h) in the case of Z^-_{bkt}, affects the accuracy of the approximation. We do note, however, that for all instances, the procurement strategy we obtain from solving $(\mathcal{U})$ yields a feasible completion to the resulting mixed integer nonlinear problem for a 24-hour instance. Longer horizons result in tractability (but not necessarily feasibility) issues.

Table 10: An analysis of the linearized constraints in $(\mathcal{U})$ versus the nonlinear constraints in $(\mathcal{P})$. Positive values represent an over-estimation, while negative values represent an under-estimation.

	Purchased Battery[1]	**Discharge**[2] ($\max_{b\in\mathcal{B},k\in\bar{\mathcal{B}}_b,t\in\mathcal{T}} \delta^-_{bkt}$)	**Charge**[3] ($\max_{b\in\mathcal{B},k\in\bar{\mathcal{B}}_b,t\in\mathcal{T}} \delta^+_{bkt}$)	**Percent of Demand**[4] ($\max_{b\in\mathcal{B},k\in\bar{\mathcal{B}}_b} \hat{d}^p_{bk}$)	**Lifecycle Approximation**[5] ($\max_{b\in\mathcal{B},k\in\bar{\mathcal{B}}_b} \delta^l_{bk}$)
Bagram	b_2	2.30	-0.80	0.031	90
Bamako	b_4	1.15	-0.40	0.050	99
Boston	b_3	1.73	-0.60	0.004	70
Brazzaville	b_5	0.58	-0.20	0.005	71
Buenos Aires	b_3	1.73	-0.60	0.030	76
Dili	b_5	0.57	-0.20	-0.004	69
Dushanbe	b_2	2.23	-0.80	0.010	67
Gangneung	b_2	2.33	-0.80	0.023	72
Istanbul	b_2	2.31	-0.80	0.024	74
Kuwait	b_3	1.73	-0.60	0.033	78
Mexico City	b_4	1.16	-0.40	0.025	79
San Salvador	b_5	0.57	-0.20	0.006	71
Springfield	b_1	2.89	-1.00	0.021	71
Tallinn	b_3	1.74	-0.60	0.013	76

[1] **Purchased Battery** details the type of battery purchased as part of the procurement solution for each instance.
[2] **Discharge** represents the difference between the actual and theoretical power discharged by the battery in kWs (over-approximation ≥ 0) per Equation (26).
[3] **Charge** represents the difference between the actual and theoretical power received by the battery in kWs (under-approximation ≤ 0) per Equation (27).
[4] **Percent of Demand** is the sum of the quotient of the difference of total amount of batter power over-estimated minus the total amount underestimated and the demand over the time horizon per Equation (28).
[5] **Lifecycle Approximation** represents the quotient of the theoretical and actual total lifecycles per Equation (29).

5 Conclusions

We present an optimization model that determines the procurement and dispatch strategy for a year-long demand profile at hourly time fidelity. Our formulation handles up to three choices of battery technologies. We use fourteen year-long demand profiles at the hourly fidelity for FOBs located in different climate zones, and solve all instances using a mixed-integer, linear approximation of the mixed-integer nonlinear program well within a time limit of 10 hours to an optimality gap of less than 5% for a prescribed set of technologies; using a heuristic warm start reduces solution times to within under an hour in most instances we test. Results suggest a hybrid system such as ours reduces fuel consumption 30%, on average, compared to a generator-only solution. Our solutions indicate a design and dispatch strategy that charges the battery when demand is low and then discharges the battery to prevent operating generators at a low-power rating. The implicit benefit of this strategy is that generators maintain levels greater than 30% of their rated power, on average, 96% of the time they are in use.

We evaluate the quality of our approximation by comparing solutions from $(\mathcal{U})$ against the nonlinear representations of power and lifecycle variables in $(\mathcal{P})$. We find that although our model overestimates battery discharge power, especially at low SOCs, the total quantity over-estimated is less than 0.02% of the total demand. This approximation error stems from the bounds on SOC, which are 0 and 1 (see Section 4.4). Bounds associated with partitioning on SOC or applying operational logic could reduce this error; however, it may be at the expense of increased solve times and/or reduced solution quality.

Rather than minimizing costs, our model could easily incorporate objectives such as minimizing environmental impact or total volume of the technologies procured. The battery parameter calculations employed for our model are applicable to other chemistries, such as lead acid and nickel cadmium. Because our model solves for both current and voltage, results from $(\mathcal{U})$ would be useful in relating design and dispatch solutions to more detailed dispatch and power flow models that consider finer-grain time fidelity. Specifically, future work entails determining dispatch decisions at minute-level fidelity by fixing the design decisions and introducing greater operational detail, including: (i) ramp-up and ramp-down time of generators, (ii) minimum up- and down-time of generators, (iii) rules of thumb by which some controls systems operate, and (iv) more accuracy in battery performance, e.g., performance factors as a function of temperature. Such a model is designed to operate using a one- to two-day "look-ahead" window, consisting of between 1,440 and 2,880 time periods. While the number of variables would be smaller than in $(\mathcal{P})$ because of the fixed procurement decisions, the minute-fidelity model contains more constraints. An alternative approach would use our strategies that determine the design influenced by a coarse dispatch strategy, and then simulate the dispatch using a rolling-horizon approach; a drawback results from the inability to obtain gradients with respect to the design variables out of that simula-

tion, so we would have to use derivative-free optimization techniques. Another extension of our model, possibly addressed through the simulation approach, would allow for the construction of a stochastic program to incorporate the variability of both solar irradiance and power demand.

Acknowledgements The authors would like to thank Dr. Mark Spector, Office of Naval Research (ONR) for full support of this research effort under contract award #N000141310839. We appreciate the consult of Dr. Paul Kohl of Georgia Tech, on whom we relied on heavily for battery expertise. We are also grateful to Evan Jones and Kimberly Fowler, Pacific Northwest National Lab (PNNL), for providing the FOB load data from EnergyPlus. Thanks is due to Gavin Goodall for his help in conducting model runs. Lastly, we acknowledge the support of the National Renewable Energy Lab (NREL) for its involvement in this project, particularly in addressing PV applications and specifically to Stephen Frank for helpful comments on prior versions of this paper.

References

1. A123 battery manufacturer. http://www.a123systems.com/. Accessed: 2015-03-15.
2. CPLEX 12. http://www.gams.com/dd/docs/solvers/cplex/. Accessed: 2015-03-15.
3. Fuel Consumption for Diesel Generators. http://greenmountaingenerators.com/2012/09/. Accessed: 2015-07-10.
4. Intelligent Power Management Distribution System (IPMDS). http://www.dtic.mil/ndia/2011power/Session2_12093_Whitmore.pdf. Accessed: 2015-05-27.
5. Power Distribution Illumination System Electrical (PDISE). http://www.fidelitytech.com/military-and-aerospace-manufacturing/products-and-services/pdise/. Accessed: 2015-05-27.
6. EnergyPlus: creating a new-generation building energy simulation program. *Energy and Buildings*, 33(4):319 – 331, 2001.
7. Army TM 9-6150-226-13. http://www.liberatedmanuals.com/TM-9-6150-226-13.pdf, 2008. Accessed: 2015-05-27.
8. Micropower system modeling with HOMER. http://homerenergy.com, 2015. Accessed 08/18/2015.
9. C. Abbey and G. Joos. Energy management strategies for optimization of energy storage in wind power hybrid system. In *Power Electronics Specialists Conference, 2005. PESC'05. IEEE 36th*, pages 2066–2072. IEEE, 2005.
10. C. Abbey and G. Joos. A stochastic optimization approach to rating of energy storage systems in wind-diesel isolated grids. *Power Systems, IEEE Transactions on*, 24(1):418–426, 2009.
11. N. Achaibou, M. Haddadi, and A. Malek. Modeling of lead acid batteries in PV systems. *Energy Procedia*, 18:538–544, 2012.
12. I. Androulakis, C. Maranas, and C. Floudas. αBB: A global optimization method for general constrained nonconvex problems. *Journal of Global Optimization*, 7(4):337–363, 1995.
13. M. Ashari and C. Nayar. An optimum dispatch strategy using set points for a photovoltaic (PV) diesel and battery hybrid power system. *Solar Energy*, 66(1):1 – 9, 1999.
14. S. Ashok. Optimised model for community-based hybrid energy system. *Renewable Energy*, 32(7):1155 – 1164, 2007.
15. B. Bala and S. Siddique. Optimal design of a PV-diesel hybrid system for electrification of an isolated island in Sandwip, Bangladesh using a genetic algorithm. *Energy for Sustainable Development*, 13(3):137 – 142, 2009.
16. T. Barbier, M. Anjos, and G. Savard. Optimization of diesel, wind, and battery hybrid power systems. Submitted, 2014.
17. C. D. Barley and C. B. Winn. Optimal dispatch strategy in remote hybrid power systems. *Solar Energy*, 58(46):165 – 179, 1996.
18. P. Belotti. Couenne: a user's manual. Technical report, Lehigh University, 2009.

19. J. L. Bernal-Agustin, R. Dufo-Lopez, and D. M. Rivas-Ascaso. Design of isolated hybrid systems minimizing costs and pollutant emissions. *Renewable Energy*, 31(14):2227 – 2244, 2006.
20. P. Bonami, L. T. Biegler, A. R. Conn, G. Cornuéjols, I. E. Grossmann, C. D. Laird, J. Lee, A. Lodi, F. Margot, and N. Sawaya. An algorithmic framework for convex mixed integer nonlinear programs. *Discrete Optimization*, 5(2):186–204, 2008.
21. A. Brooke, D. Kendrick, and A. Meeraus. *GAMS – A User's Guide (Release 2.25)*. Boyd & Fraser Publishing Company, Danvers, Massachusetts, 1992.
22. J. Copetti and F. Chenlo. Lead acid batteries for photovoltaic applications: Test results and modeling. *Journal of Power Sources*, 47(1):109–118, 1994.
23. A. P. Dobos. PVWatts Version 1 technical reference. *National Renewable Energy Laboratory, Report Number TP-6A20-60272*, 2013.
24. D. Doerffel and S. A. Sharkh. A critical review of using the Peukert equation for determining the remaining capacity of lead-acid and lithium-ion batteries. *Journal of Power Sources*, 155(2):395–400, 2006.
25. R. Dufo-Lopez and J. L. Bernal-Agustin. Design and control strategies of PV-diesel systems using genetic algorithms. *Solar Energy*, 79(1):33 – 46, 2005.
26. R. Dufo-López, J. M. Lujano-Rojas, and J. L. Bernal-Agustín. Comparison of different lead–acid battery lifetime prediction models for use in simulation of stand-alone photovoltaic systems. *Applied Energy*, 115:242–253, 2014.
27. M. Engels, P. A. Boyd, T. M. Koehler, S. Goel, D. R. Sisk, D. D. Hatley, V. V. Mendon, and J. C. Hail. Smart and Green Energy (SAGE) for base camps final report. Technical report, Pacific Northwest National Laboratory (PNNL), Richland, WA (US), 2014.
28. I. J. Fernndez, C. F. Calvillo, A. Sanchez-Miralles, and J. Boal. Capacity fade and aging models for electric batteries and optimal charging strategy for electric vehicles. *Energy, Sustainability and Society*, 60:35–43, 2013.
29. A. Flores-Tlacuahuac and L. T. Biegler. A robust and efficient mixed-integer non-linear dynamic optimization approach for simultaneous design and control. *Computer Aided Chemical Engineering*, 20:67–72, 2005.
30. L. Gao, S. Liu, and R. A. Dougal. Dynamic lithium-ion battery model for system simulation. *IEEE: Transactions on Components and Packaging Technologies*, 25(3):495–505, 2002.
31. T. Givler and P. Lilienthal. Using HOMER software, NREL's micropower optimization model, to explore the role of gen-sets in small solar power systems. Technical Report NREL/TP-710-36774, National Renewable Energy Laboratory, May 2005.
32. H. Gooi, D. Mendes, K. Bell, and D. Kirschen. Optimal scheduling of spinning reserve. *Power Systems, IEEE Transactions on*, 14(4):1485–1492, 1999.
33. F. Huneke, J. Henkel, J. A. B. González, and G. Erdmann. Optimisation of hybrid off-grid energy systems by linear programming. *Energy,*

Sustainability and Society, 2(1):1–19, 2012.
34. M. R. Jongerden and B. R. Haverkort. Which battery model to use? *Software, IET*, 3(6):445–457, 2009.
35. M. Jun, K. Smith, E. Wood, and M. C. Smart. Battery capacity estimation of low-earth orbit satellite application. *International Journal of Prognostics and Health Management*, 3:81, 2012.
36. S. Kamel and C. Dahl. The economics of hybrid power systems for sustainable desert agriculture in Egypt. *Energy*, 30(8):1271 – 1281, 2005.
37. Y. Katsigiannis and P. Georgilakis. Optimal sizing of small isolated hybrid power systems using tabu search. *Journal of Optoelectronics and Advanced Materials*, 10(5):1241, 2008.
38. E. Koutroulis, D. Kolokotsa, A. Potirakis, and K. Kalaitzakis. Methodology for optimal sizing of stand-alone photovoltaic-wind-generator systems using genetic algorithms. *Solar Energy*, 80(9):1072 – 1088, 2006.
39. J. F. Manwell and J. G. McGowan. Lead acid battery storage model for hybrid energy systems. *Solar Energy*, 50(5):399–405, 1993.
40. V. Marano, S. Onori, Y. Guezennec, G. Rizzoni, and N. Madella. Lithium-ion batteries life estimation for plug-in hybrid electric vehicles. *IEEE Vehicle and Power Propulsion Conference*, pages 536–543, 2009.
41. N. C. McCaskey. Renewable energy systems for forward operating bases: A simulations-based optimization approach. Technical report, Colorado State University, 2010.
42. G. P. McCormick. Computability of global solutions to factorable nonconvex programs: Part I: Convex underestimating problems. *Mathematical Programming*, 10(1):147–175, 1976.
43. H. Morais, P. Kadar, P. Faria, Z. A. Vale, and H. Khodr. Optimal scheduling of a renewable micro-grid in an isolated load area using mixed-integer linear programming. *Renewable Energy*, 35(1):151 – 156, 2010.
44. M. A. Ortega-Vazquez and D. S. Kirschen. Optimizing the spinning reserve requirements using a cost/benefit analysis. *Power Systems, IEEE Transactions on*, 22(1):24–33, 2007.
45. M. A. Ortega-Vazquez and D. S. Kirschen. Estimating the spinning reserve requirements in systems with significant wind power generation penetration. *Power Systems, IEEE Transactions on*, 24(1):114–124, 2009.
46. K. A. Pruitt, R. J. Braun, and A. M. Newman. Evaluating shortfalls in mixed-integer programming approaches for the optimal design and dispatch of distributed generation systems. *Applied Energy*, 102:386–398, 2013.
47. Y. Rebours and D. Kirschen. What is spinning reserve? *The University of Manchester*, pages 1–11, 2005.
48. S. Rehman and L. M. Al-Hadhrami. Study of a solar PV diesel battery hybrid power system for a remotely located population near Rafha, Saudi Arabia. *Energy*, 35(12):4986 – 4995, 2010.
49. G. Rossum. Python reference manual. Technical report, Amsterdam, The Netherlands, The Netherlands, 1995.

50. N. V. Sahinidis. BARON: A general purpose global optimization software package. *Journal of Global Optimization*, 8:201–205, 1996.
51. M. S. Scioletti, J. K. Goodman, P. A. Kohl, and A. M. Newman. A physics-based integer-linear battery modeling paradigm. *Applied Energy*, 176:245–257, 2016.
52. SERDP. Sustainable forward operating bases. `https://www.serdp-estcp.org/content/download/.../FOB_Report_Public.pdf`, 2010.
53. S. Shaahid and I. El-Amin. Techno-economic evaluation of off-grid hybrid photovoltaic diesel battery power systems for rural electrification in Saudi Arabia as a way forward for sustainable development. *Renewable and Sustainable Energy Reviews*, 13(3):625 – 633, 2009.
54. H. D. Sherali and J. C. Smith. Improving discrete model representations via symmetry considerations. *Management Science*, 47(10):1396–1407, 2001.
55. J. Vavrin. Power and energy considerations at forward operating bases. `http://e2s2.ndia.org/pastmeetings/2010/tracks/Documents/9874.pdf`, 2010.
56. J. Wang, J. H.-G. P. Liu, E. Sherman, S. Soukiazian, M. Verbrugge, H. Tataria, J. Musser, and P. Finamore. Cycle-life model for graphite-LiFePO4 cells. *Power Sources*, 196(8):3942–3948, 2011.

Appendix

Algorithm 3 Attempts to determine a myopic dispatch strategy for a given design decision: a set of generators $g \in \mathcal{G}$ and their twins $k \in \tilde{\mathcal{G}}_g$, batteries $b \in \mathcal{B}$ and their twins $k \in \tilde{\mathcal{B}}_b$, and PV systems $s \in \mathcal{S}$ in the design, with $\tilde{\mathcal{G}}_g$ and $\tilde{\mathcal{B}}_b$ provided by Algorithms 1 and 2, respectively. Let $g \in \hat{\mathcal{G}}$ denote the set of all generators in the design decision, including twins, in decreasing order by rated capacity.

procedure $\mathcal{H}^1$
  $t \leftarrow 1$
  while $t \leq |\mathcal{T}|$ **do**
    $Res_t \leftarrow \sum_{s \in \mathcal{S}} \gamma_{st} k^s X_s$ ▷ spinning reserve requirement, if using max PV
    $Load_t \leftarrow (1 + \bar{k}) d_t^P$ ▷ load requirement
    $G_{gt} \leftarrow 0, \ \forall g \in \hat{\mathcal{G}}$ ▷ all generators are off to start; $\hat{\mathcal{G}}$ ordered by max output
    $Gen_t \leftarrow 0$ ▷ capacity of generators that are turned on
    $BOut_t \leftarrow \eta_b^- \cdot (a_b^v B_{b,t-1}^{soc} + b_b^v - i_b^{avg} r_b^{int}) \cdot \min \left\{ i_b^{U-}, \frac{c_b^{ref}}{c_b^- + \tau} B_{b,t-1}^{soc} \right\}$ ▷ max discharge
    $BIn_t \leftarrow \frac{(a_b^v B_{b,t-1}^{soc} + b_b^v + i_b^{avg} r_b^{int}) \min \left\{ i_b^{U+}, \frac{c_b^{ref}}{c_b^+}, \frac{c_b^{ref}(1 - B_{b,t-1}^{soc})}{\tau} \right\}}{\eta_b^+}$ ▷ max charge
    $BRes_t \leftarrow \eta_b^- \bar{p}_b B_{b,t-1}^{soc}$ ▷ spinning reserve from idle battery
    $PV_t \leftarrow \sum_{s \in \mathcal{S}} \gamma_{st} X_s$ ▷ maximum PV power output
    while $Gen_t + BOut_t + PV_t < Load_t$ **or** $Gen_t - (Load_t - PV_t) + BRes_t < Res_t$ **do**
      $\hat{g} \leftarrow \max\{g \in \hat{\mathcal{G}} : G_{gt} = 0\}$
      if $G_{\hat{g}-1,t} = 0$ **then**
        $G_{\hat{g}-1,t} \leftarrow 1$ ▷ turn off smallest running generator
        $G_{\hat{g}t} \leftarrow 0 \ Gen_t \leftarrow Gen_t - \eta_{\hat{g}}^- \bar{p}_{\hat{g}} + \eta_{\hat{g}-1}^- \bar{p}_{\hat{g}-1}$ ▷ turn on next smallest
      else if $G_{|\hat{G}|t} = 0$ **then** ▷ turn on smallest running generator
        $G_{|\hat{G}|t} \leftarrow 1; \ Gen_t \leftarrow Gen_t + \eta_{|\hat{G}|}^- \bar{p}_{|\hat{G}|}$
      else return *Infeasible* ▷ all generators on, load or spinning reserve unmet
    if $PV_t > Load_t + BIn_t$ **then** ▷ use only PV, max charge battery
      $\sum_{s \in \mathcal{S}} P_{st}^{PV} \leftarrow Load_t + BIn_t; \ P_{bt}^- \leftarrow 0; \ P_{bt}^+ \leftarrow BIn_t; \ P_{gt}^- \leftarrow 0 \ \forall g \in \hat{\mathcal{G}}$

else if $PV_t + Gen_t > Load_t + BIn_t$ **then** ▷ max charge battery

$P_{st}^{PV} \leftarrow \gamma_{st} X_s \ \forall s \in \mathcal{S};\ P_{bt}^{-} \leftarrow 0$

$P_{bt}^{+} \leftarrow BIn_t;\ \sum_{g \in \hat{\mathcal{G}}} P_{gt}^{-} \leftarrow Load_t + BIn_t - PV_t$

else if $PV_t + Gen_t > Load_t$ **then** ▷ charge battery

$P_{st}^{PV} \leftarrow \gamma_{st} X_s \ \forall s \in \mathcal{S};\ P_{bt}^{-} \leftarrow 0$

$P_{bt}^{+} \leftarrow PV_t + Gen_t - Load_t;\ P_{gt}^{-} \leftarrow \bar{p}_g G_{gt} \ \forall g \in \hat{\mathcal{G}}$

else ▷ discharge battery

$P_{st}^{PV} \leftarrow \gamma_{st} X_s \ \forall s \in \mathcal{S};\ P_{bt}^{-} \leftarrow \frac{(Load_t - PV_t - Gen_t)}{\eta_b^{-}};\ P_{bt}^{+} \leftarrow 0$

$P_{gt}^{-} \leftarrow \bar{p}_g G_{gt} \ \forall g \in \hat{\mathcal{G}}$

$B_{bt}^{soc} \leftarrow B_{b,t-1}^{soc} + \frac{P_{bt}^{+}}{c_b^{ref}(a_b^v B_{b,t-1}^{soc} + b_b^v + i_b^{avg} r_b^{int})} - \frac{P_{bt}^{-}}{c_b^{ref}(a_b^v B_{b,t-1}^{soc} + b_b^v - i_b^{avg} r_b^{int})}$ ▷ update battery SOC

$t \leftarrow t + 1$ ▷ continue until time horizon completed or infeasible

return $P_{st}^{PV} \ \forall s \in \mathcal{S}, t \in \mathcal{T};\ P_{bt}^{+} \ \forall t \in \mathcal{T};\ P_{bt}^{-} \ \forall t \in \mathcal{T};\ P_{gt}^{-} \ \forall g \in \hat{\mathcal{G}}, t \in \mathcal{T};$

$B_{bt}^{soc} \ \forall t \in \mathcal{T};\ G_{gt} \ \forall g \in \hat{\mathcal{G}}, t \in \mathcal{T}$ ▷ calculate cost